



# Geomechanical Behaviour of Clay Stabilised with Low-Calcium Fly Ash and Alkali Activation

Canan Turan<sup>1</sup> · Akbar A. Javadi<sup>2</sup> ·  
Raffaele Vinai<sup>2</sup> · Ibrahim Oz<sup>1</sup>

Received: 28 March 2025 / Accepted: 14 July 2025 / Published online: 2 August 2025  
© The Author(s), under exclusive licence to Indian Geotechnical Society 2025

**Abstract** This study examines the geomechanical behaviour of clay stabilised with alkali-activated fly ash and non-activated fly ash to improve the geotechnical properties of clay soils. Class F fly ash and its alkali-activated form were employed as stabilisers to provide a sustainable alternative to traditional binders like cement and lime. Laboratory experiments, including one-dimensional consolidation and consolidated-undrained triaxial tests, were conducted on clay samples treated with varying fly ash contents and curing durations. The results indicated that alkali-activated fly ash significantly improved the mechanical performance of clay by reducing compressibility, swelling, and permeability during curing. Triaxial test results showed that alkali activation increased strength parameters and altered the stress–strain behaviour of the soil from ductile to brittle. Specifically, clay treated with 25% alkali-activated fly ash and cured for 28 days achieved nearly a ninefold increase in maximum deviator stress compared to untreated samples. Both fly ash types improved shear strength and critical state parameters, though non-activated fly ash resulted in lower effective cohesion than the control. Overall, the findings demonstrate that untreated Class F fly ash has limited binding capacity, while

alkali activation substantially enhances the stabilisation effect, offering a promising and sustainable alternative for geotechnical soil improvement.

**Keywords** Soil stabilisation · Clay · Fly ash · Alkali activation · Consolidation · Triaxial test

## Introduction

Utilisation of clay soils in geotechnical engineering projects is typically limited due to their low strength and high compressibility properties, which usually cause differential settlements [1]. Hence, stabilisation methods are required to improve the clay properties. Chemical stabilisation is one of the common engineering treatments, as it provides enhanced interfacial strength between soil particles and binders [2, 3]. Ordinary Portland cement (OPC) and lime are the most common chemical binders used to stabilise soil [4]. However, utilisation of cement or lime as a binder is becoming unsustainable owing to the greenhouse gas emissions like carbon dioxide (CO<sub>2</sub>) and nitric oxide (NO<sub>x</sub>) associated to their manufacturing process [5, 6]. The manufacture of OPC is estimated to cause approximately 7–10% of global CO<sub>2</sub> emissions annually [7–9]. Therefore, environmentally friendly binders have been investigated by many researchers to decrease environmental impacts and to compete with OPC or lime [6, 7]. Industrial byproduct such as fly ash has been used as alternative binder due to its low-emission properties; however, insufficient mechanical properties have been reported by using only fly ash (specifically class F) in comparison with cement. Hence, geopolymers, ‘synthetic alkali aluminosilicates’ [10], have been recently proposed as innovative binders due to their lower impact and good mechanical properties [6, 7, 10–12]. Geopolymers demonstrated

✉ Canan Turan  
canan.turan@ahievran.edu.tr

Akbar A. Javadi  
a.a.javadi@exeter.ac.uk

Raffaele Vinai  
r.vinai@exeter.ac.uk

Ibrahim Oz  
ibrahim.oz@ahievran.edu.tr

<sup>1</sup> Department of Civil Engineering, Kirsehir Ahi Evran University, 40100 Kirsehir, Turkey

<sup>2</sup> Department of Engineering, University of Exeter, Exeter EX4 4QF, UK

better resistance to chemical degradation such as chloride, sulphate, and acid attacks than cement-based binders, hence improving the durability of the materials [13].

Geopolymers are reaction products of alkali-activated aluminosilicate materials [14, 15]. Fly ash is the most commonly used aluminosilicate-based material for making geopolymer [10]. Recently, utilisation of fly ash has become popular as a precursor to form geopolymer since large amount of fly ash is available in worldwide stockpiles [16, 17]. Also, improper disposal of fly ash can cause ground water, surface water, and air pollution due to the leaching of its toxic trace elements to underground water, deep and surface soil [4], yet, these toxic trace elements can be trapped and immobilised in geopolymer matrix [14, 18, 19]. Fly ash-based geopolymer is mainly produced by alkali-activated geopolymerisation process under mild temperatures [14]. Geopolymerisation occurs through a process involving the dissolution of aluminium (Al) and silicon (Si) species in a highly alkaline environment, thereafter transportation or orientation of dissolved species into monomers, followed by the polymerisation/polycondensation of monomers into polymeric structure/3-dimensional aluminosilicate network [16, 17, 20]. The process can be explained in detail in the following steps. Firstly, the Si–O–Si, Al–O–Al, and Al–O–Si covalent bonds present an original amorphous aluminosilicate microstructure in the precursor (fly ash) are dissolved by the high hydroxyl ( $\text{OH}^-$ ) concentration under the alkali conditions. After releasing Al and Si ions into the solution, the alkali cations (generally  $\text{Na}^+$  or  $\text{K}^+$ ) compensate the excess negative charges to modify of the aluminium coordination under the dissolution process. Subsequently, the resulting products precipitate and reorganise into repeated structure Si–O–Al and Si–O–Si bonds and become more stable [13]. When the calcium is the majority in the precursor, the calcium–aluminium–silicate–hydrate (CASH) gel is produced as the main reaction product [11]. In another case, the Si and Al ions are collected around the nuclei points, shared the oxygen ions, and formed as a Si–O–Al and Si–O–Si three-dimensional polymeric chain. The reaction product which is an amorphous aluminosilicate gel is evolved to a Si-rich phase from an Al-rich phase. In some scenarios, crystallisation process can be observed with curing time and high temperature after the precipitation and the gel gets harden, in this case, zeolite like polymers is produced [13].

The type and concentration of precursors and alkali activators play an important role in geopolymerisation process [11, 14, 21, 22]. Precursors rich in Si and Al are the primary requirements for geopolymerisation [16]. Fly ash includes adequate  $\text{SiO}_2$  and  $\text{Al}_2\text{O}_3$  in amorphous phase, and it gives an effective reaction with alkali activators [6]. Fly ash can be divided into 2 types according to ASTM C618 standards which are class C and class F [23]. Class C fly ash includes between 50 and 70% amount of  $\text{SiO}_2$ ,  $\text{Al}_2\text{O}_3$ , and

$\text{Fe}_2\text{O}_3$ , whereas class F fly ash includes over 70% amount of  $\text{SiO}_2$ ,  $\text{Al}_2\text{O}_3$ , and  $\text{Fe}_2\text{O}_3$ . Therefore, class F fly ash is recommended as a precursor in comparison with class C fly ash for higher geopolymerisation [6, 24, 25]. The type and dosage of alkali activators significantly affect the dissolution of  $\text{Si}^{4+}$  and  $\text{Al}^{3+}$  from precursor during geopolymerisation [14, 19]. Releasing of  $\text{Si}^{4+}$  and  $\text{Al}^{3+}$  is generally higher with sodium-based solutions compared to potassium-based solutions [16, 26]. Singh et al. [27] carried out heavy compaction and unconfined compressive strength (UCS) tests on fly ash using sodium hydroxide and potassium hydroxide separately and they found out that the strength parameters are higher with sodium hydroxide compared to potassium hydroxide. Also, potassium-based solutions are not commonly used as they have cost limitations, hence sodium-based solutions are highly recommended to utilise as the alkali activators [25]. It has also been deduced that reactions take place at a higher rate when using the combination of sodium silicate and sodium hydroxide instead of using only sodium hydroxide [6, 16]. This is because available free Si in the activating sodium silicate solution can improve the polycondensation reaction during geopolymerisation process.

The utilisation of sodium silicate (SS) and/or sodium hydroxide (SH) solution with fly ash to stabilise soil has recently been investigated as an innovative solution to decrease cement production by many researchers e.g. 5, 7, 13, 28–36. Rios et al. [13] showed that silty sand stabilised with 20% fly ash and an SS/SH mass ratio of 1/2 showed significant improvements in UCS. The alkali activator solution was applied at 11.7% to 19.5% by weight, with the highest UCS observed at lower solution content (11.7%). Long-term curing led to a substantial increase in UCS, with the reaction mechanism being slower but more durable compared to soil–cement mixtures. Ridtirud et al. [32] also reported optimal UCS results for silty clayey gravel with a 1/1 SS/SH ratio at room temperature and a 2/3 ratio at 40 °C. Other studies supported these findings by studying different soil types, activator ratios, and fly ash contents. Murmu et al. [5] found that black cotton soil stabilised with 5–20% fly ash and an SH concentration of 5 M improved strength and reduced plasticity, with optimal results at 10% fly ash. Similarly, Trinh and Bui [33] examined class F fly ash with an SS/SH ratio of 2 and an activator solution/fly ash ratio of 0.5, showing that compressive strength increased. Meanwhile, Abdullah et al. [37] and Syed et al. [36] emphasised that the SS/SH and alkali solution/fly ash ratios significantly affected durability, plasticity, and swelling characteristics, with improvements in UCS and the formation of aluminosilicate gels confirmed through SEM and XRD analyses.

Recent studies have also confirmed that alkali-activated binders significantly enhance the mechanical and volumetric behaviour of clayey soils. Miao et al. [38] investigated the stabilisation of expansive black cotton soil using volcanic

ash-based geopolymers and reported substantial reductions in plasticity and swelling, and a UCS of 16.55 MPa was achieved after 90 days of curing. Khadka et al. [39] synthesised and modified fly ash- and metakaolin-based geopolymers using lime and gypsum, and found that gypsum-modified geopolymers were more effective in reducing swelling in high-plasticity clay, with optimum results achieved at 6.0–9.5% additive content. Debanath et al. [40] demonstrated that class F fly ash-based geopolymer binders substantially enhance the strength and reduce the swelling potential of expansive soils, with 20% binder content mitigating swelling pressure and increasing UCS by up to 400% after 28 days of curing. Dudekula et al. [41] examined the stabilisation of expansive clayey sand using 10% GGBS and a 1.0-M geopolymer solution, reporting a 238% increase in UCS and a 90% reduction in swelling pressure.

It is evident that majority of previous studies in soil stabilisation found in the literature used the ratio of SS/SH and alkali activator solution/fly ash to indicate the amount of alkali activators [28–33]. However, many researchers in geopolymer studies emphasised the importance of silica modulus (SM) and alkali dosages (M+) e.g. 18, 42–45. Gado et al. [46] and Firdous and Stephan [47] indicated that the variation of SM considerably affects the polymerisation degree of dissolved aluminate and silicate species in solution; in this way, the geopolymer structure can be affected with different SM. Krizan and Zivanovic [43] also argued that the hydration level is modified by sodium content (M+) and SM. Yusuf et al. [45] showed that the commercially available SS solutions have different initial SM ratios. Thus, using effective or optimum SM in tests is more appropriate for obtaining the required strength compared with evaluating only the ratio of SS/SH.

Previous studies also showed enhanced results in terms of UCS, CBR, durability, and microstructure of soils stabilised with alkali-activated fly ash. The literature revealed that the UCS test is widely used due to its simplicity in assessing the strength properties of stabilised soils. However, the UCS test has limitations in precisely predicting load-deformation responses due to the inability to control drainage conditions. In contrast, the triaxial test replicates the effects of confining pressure and pore water pressure, which are crucial for determining strength parameters. Despite this, only a few studies have extended the use of advanced testing such as consolidated triaxial and consolidation tests to evaluate the performance of alkali-activated fly ash in clayey soils, limiting our understanding of their applicability in real field scenarios. Thus, there is a lack of study on triaxial, and consolidation behaviour of soil stabilised with alkali-activated fly ash including stress–strain behaviour, undrained shear strength, and consolidation characteristics and the limited literature is generally focused on stabilising sand instead of clay [13, 48]. Detailed studies involving triaxial testing

and critical state line analysis for alkali-activated fly ash-stabilised soils are therefore strongly recommended [25].

Based on the above considerations, this study aims to provide a novel perspective on clay stabilisation by evaluating the performance of alkali-activated and non-activated fly ash through advanced geotechnical testing. Specifically, it addresses a significant gap in the literature by investigating the effects of alkali activation on the mechanical and consolidation behaviour of clay, which has received limited attention compared to sand stabilisation. While previous studies have primarily focused on strength or swelling parameters, this study offers additional insights into the mechanical and consolidation performance of clayey soils stabilised with alkali-activated fly ash, particularly under consolidated conditions that better simulate insitu field behaviour. The study incorporates a systematic approach to assess stress–strain behaviour, undrained shear strength, and consolidation characteristics via consolidated-undrained (CU) triaxial tests and one-dimensional consolidation tests conducted at 1, 7, and 28 days of curing.

In this context, the clay soil was stabilised using both non-activated and alkali-activated class F fly ash, with the activation parameters selected based on prior optimisation studies to ensure effective stabilisation. By examining the mechanical and consolidation responses of the stabilised clay, this study highlights the differences between alkali-activated and conventional fly ash stabilisation approaches. The findings aim to support the advancement of sustainable geotechnical practices by promoting the beneficial reuse of industrial by-products, thereby contributing to environmental sustainability and the circular economy.

## Materials and Method

### Materials

The soil used in this study was a commercial China clay. It had a liquid limit of 49%, plastic limit of 25%, and plasticity index of 24% and was classified as clay with intermediate plasticity (CI), based on the British standard, BS EN ISO 14688-2 [49]. The results of Standard Proctor tests indicated that the soil had a maximum dry unit weight ( $\gamma_{dmax}$ ) of 15.2 kN/m<sup>3</sup> at optimum moisture content ( $w_{opt}$ ) of 21%. Specific gravity of solid particles was measured equal to 2.6 according to the small pycnometer test. The average chemical (oxide) composition of kaolinite, determined using X-ray fluorescence (XRF) analysis, is presented in Table 1. A Loss on Ignition (LOI) value of 11.7% was measured for the synthetic kaolin. Khaled et al. [50] reported a similar value of 11.65% and argued that this reflects the expected dehydroxylation behaviour of kaolinite.

**Table 1** Oxide compositions of clay and low-calcium class F fly ash

Chemical composition	Clay	Fly ash
CaO (%)	0.1	2.2
SiO <sub>2</sub> (%)	54.8	48.6
Al <sub>2</sub> O <sub>3</sub> (%)	31.1	22.5
Fe <sub>2</sub> O <sub>3</sub> (%)	1.0	9.2
K <sub>2</sub> O (%)	2.1	4.1
MgO (%)	0.4	1.3
Na <sub>2</sub> O (%)	0.1	0.9
P <sub>2</sub> O <sub>5</sub> (%)	0.1	0.2
SO <sub>3</sub> (%)	/	0.9
TiO <sub>2</sub> (%)	0.1	1.1
LOI (%)	11.7	3.6

Class F fly ash utilised in this study was obtained from Power Minerals Ltd, UK. Due to its predominantly silt-sized particle distribution, the plasticity characteristics of the fly ash could not be established, and it was classified as non-plastic (NP). The specific gravity of the material, determined using the small pycnometer method, was measured as 2.32. The average oxide composition of the fly ash, determined using XRF analysis and presented in Table 1, confirms its classification as class F in accordance with ASTM C618 [51].

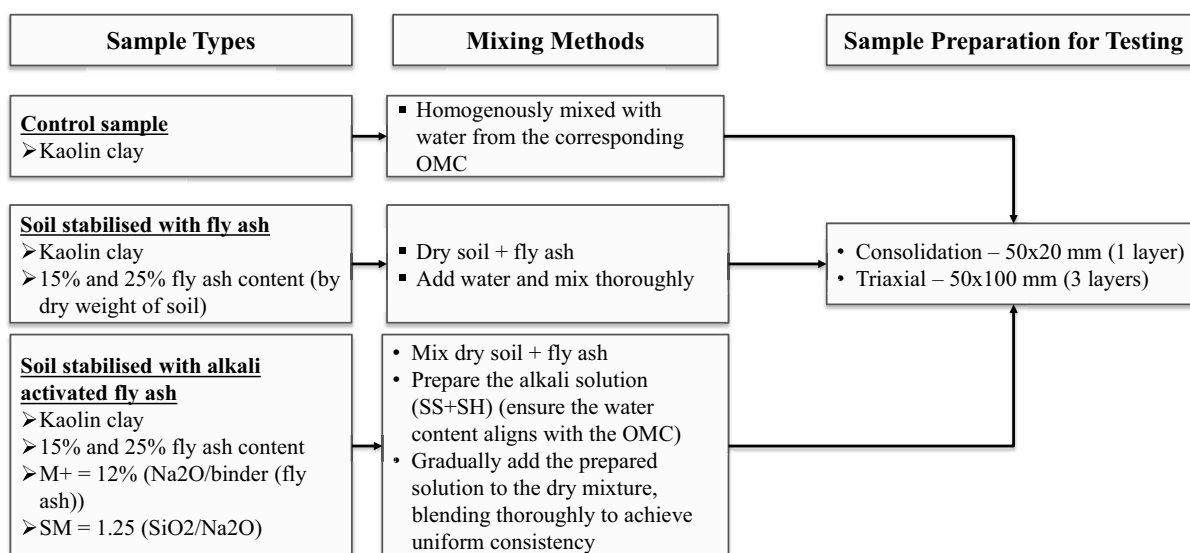
Commercially available alkali activators were used in the study. Laboratory grade sodium hydroxide pellets of 99% purity were used. Sodium silicate solution was sourced from Fisher Scientific UK Ltd in liquid form, composed of 14% Na<sub>2</sub>O, 28% SiO<sub>2</sub>, and 58% H<sub>2</sub>O, by weight.

## Sample preparation

The key steps of the sample preparation process are outlined in Fig. 1. The control sample (kaolin soil) and the soil samples stabilised with 15% and 25% class F fly ash content based on weight of the dry soil were prepared according to their respective optimum moisture content (OMC) as obtained from Standard Proctor tests.

For soils stabilised with alkali-activated class F fly ash, the activator ratios—silica modulus (SM) and alkali dosage (M+) were held constant for both 15% and 25% fly ash contents. The M+ value represents the mass ratio (in %) of total sodium oxide (Na<sub>2</sub>O) from both sodium silicate (SS) and sodium hydroxide (SH) solutions to the mass of fly ash binder [52–54]. SM refers to the mass ratio of SiO<sub>2</sub> to Na<sub>2</sub>O in the activating solution.

Very low or high values of M+ and SM have been reported as unsuitable for achieving optimal compressive strength [18, 47, 54]. According to Turan et al. [54], compressive strength increases with rising M+ and SM values up to a certain optimum, beyond which strength begins to decline. In addition to strength considerations, the selection of an M+ content of 12% and an SM of 1.25 also reflects their importance in controlling the geopolymerisation mechanism. A silica modulus within the range of 1.2–1.4 typically provides an adequate amount of soluble silica to support the formation of a three-dimensional aluminosilicate gel network. Likewise, an M+ level of 12% ensures sufficiently alkaline environment to dissolve precursors effectively, without causing excessive mixture viscosity. Previous studies on clay soils stabilised with alkali-activated fly ash have shown

**Fig. 1** Flow chart of the sample preparation steps

that these values result in both enhanced UCS and favourable reaction kinetics [32, 54, 55].

In terms of mixing method, the dry clay soil was initially mixed with fly ash. After obtaining homogeneous mixture, the alkali activating solution (a mix of SS and SH) was added and further mixing followed. This mixing method was recommended by Leong et al. [31] to obtain higher strength parameters. SH powder was dissolved in water to obtain SH solution. For each sample of triaxial and one-dimensional consolidation test, optimum moisture content obtained from compaction test was used. The amount of water used to dissolve the SH powder was calculated reducing the water required to achieve the OMC of the sample by the water already included in the SS solution for each sample.

Specimens were statically compacted using an Instron 3382 Floor Model Universal Testing Machine. For triaxial testing, samples with dimensions of 50 mm diameter and 100 mm height were compacted in three layers within a cylindrical steel mould. For one-dimensional consolidation tests, specimens were compacted as a single layer, with dimensions of 50 mm diameter and 20 mm height. Following compaction, all samples were carefully demoulded, sealed in plastic bags, and cured in vacuum desiccators at a controlled room temperature (23–26 °C) for the designated curing durations prior to testing.

### Testing procedures

One-dimensional consolidation tests were performed on the control soil and soils treated with 15% and 25% of either low-calcium fly ash or alkali-activated fly ash. The samples were compacted at their respective OMC and placed into consolidation rings without prior artificial saturation. However, as drainage was allowed from both ends during testing, gradual water redistribution likely occurred under higher stresses, leading to partial saturation over time. This setup reflects typical field conditions where compacted soils at OMC become progressively saturated due to wetting or rising groundwater. As suggested by Mok [56], such samples can gradually approach saturation during consolidation loading. The testing procedure adhered to the British Standard BS 1377-5 [57] and was applied to samples cured for 1, 7, and 28 days. The loading sequence followed a progression of vertical stresses: 50, 100, 200, 400, 800, 1600, then unloaded to 800, 400, and 200 kPa. Drainage was permitted from both the top and bottom surfaces of the specimens, and each loading and unloading phase was maintained for a duration of 24 h.

Consolidated-undrained (CU) triaxial tests were performed in accordance with BS 1377-8 [58] on three types of specimens: untreated control samples, fly ash-stabilised soils, and soils treated with alkali-activated fly ash. Two different fly ash dosages, 15% and 25%, were evaluated.

The experiments were conducted using GDS triaxial testing equipment operated with GDS software. The standard sequence of saturation, consolidation, and shearing stages was followed, with effective confining pressures applied at 200, 400, and 600 kPa. Following the saturation process, the degree of saturation of the specimens was assessed by calculating Skempton's B-value (commonly referred to as the B-check). This involved applying an increment in cell pressure ( $\Delta\sigma_3$ ) and measuring the resulting change in pore water pressure ( $\Delta u$ ), with the B-value calculated as the ratio  $\Delta u/\Delta\sigma_3$ . While a B-value of 0.95 is generally recommended to confirm full saturation, particularly in accordance with BS 1377-8 [58], it is acknowledged that such values may be difficult to achieve in very stiff soils. In such cases, a minimum B-value of 0.90 is considered acceptable. Therefore, in this study, the saturation phase was deemed complete when the B-value fell within the range of 0.90 to 0.95. In accordance with standard CU test protocols, Skempton's B-value was measured after saturation and prior to consolidation, and values in the range of 0.90–0.95 were considered acceptable to confirm sufficient saturation before shearing.

To achieve B-values around 0.90, the specimens were saturated by applying an incremental back pressure during the saturation phase, allowing the pore spaces to be gradually filled with water. In this method, pore water pressure is progressively increased by simultaneously applying back pressure and cell pressure to the specimen. This approach is consistent with the procedures reported by Abdullah et al. [8] and Abdullah and Shahin [59], who applied incremental back pressure to fly ash-based geopolymer-treated clay samples and similarly achieved B-values close to 0.90. In addition, Ignat et al. [60] employed comparable methods in lime-cement-improved clays and reported a B-value of 0.92 under an effective confining pressure of 150 kPa. It should also be noted that the saturation period for the control specimens lasted 24 h. However, for the stabilised specimens, this duration was insufficient to achieve the target saturation level. Therefore, an extended saturation process was applied to ensure adequate saturation before consolidation and shearing.

## Results and Discussion

### One-Dimensional Consolidation Tests

To evaluate key geotechnical parameters such as the compression index ( $C_c$ ), swelling index ( $C_s$ ), pre-consolidation pressure or yield stress ( $\sigma_y$ ), and permeability ( $k$ ), one-dimensional consolidation tests were conducted on untreated soil, fly ash-stabilised specimens, and those treated with alkali-activated fly ash.

Table 2 presents the results for the compression index ( $C_c$ ) and swelling index ( $C_s$ ) obtained from tests conducted on control, fly ash-stabilised ( $F$ ), and alkali-activated fly ash-stabilised ( $F + AA$ ) samples incorporating 15% and 25% fly ash, cured for 1, 7, and 28 days. The  $C_c$  values presented in Table 2 were calculated as the slope of the virgin compression line on the  $e$ - $\log \sigma$  curve, based on oedometer test data. In this study, the  $C_c$  was computed using void ratio values corresponding to loading stages typically between 50 and 800 kPa, where the  $e$ - $\log \sigma$  relationship exhibited a clear linear trend. The point  $e_0$  in this context refers to the void ratio at the beginning of this selected linear portion—often around 50 kPa—not the initial void ratio measured before any loading. This distinction is important to ensure consistency in the interpretation of compression behaviour. Similarly, the swelling index was determined as the slope of the unloading portion of the  $e$ - $\log \sigma$  curve following the maximum applied load. Both parameters were calculated in accordance with standard geotechnical practice to reflect the compressibility and swelling behaviour of the tested soils [57]. The data showed that, at 1 day of curing,  $C_c$  increased for soil with 15% fly ash but decreased when 25% fly ash was used. This pattern aligns with findings by Phanikumar [61], who observed an initial rise followed by a decline in the  $C_c$  of clayey soils treated with class F fly ash beyond a certain dosage. Conversely, the inclusion of alkali-activated fly ash led to a notable reduction in  $C_c$ . A similar trend was noted by Mir and Sridharan [62] with class C fly ash, attributing the improvement in compressibility to the formation of calcium silicate hydrate (CSH) cementitious compounds. In the case of alkali-activated fly ash treatment, the generation of

sodium aluminosilicate hydrate (NASH) gels likely contributed to the observed decrease in compressibility. Additionally, changes in particle size distribution may have played a role; Shil and Pal [63] reported a reduction in clay-sized particles and an increase in silt-sized fractions upon the addition of fly ash, which led to improved compressibility characteristics. Furthermore, an overall decline in  $C_c$  was observed with increased curing time for both stabilisation methods, likely due to the progressive development of cementitious bonds that enhance interparticle bonding and reduce compressibility [62, 64]. In alkali-activated systems, the formation of geopolymer gels promotes particle aggregation and flocculation, enhancing soil stiffness and strength and thereby reducing compressibility [65].

As shown in Table 2, the swelling index ( $C_s$ ) consistently declined with increasing content of fly ash or alkali-activated fly ash, as well as with extended curing duration. Notably, alkali-activated fly ash demonstrated a significantly greater reduction effect on  $C_s$  compared to untreated fly ash. For instance, at 28 days of curing, the  $C_s$  value of the untreated control sample was 0.048, which reduced to 0.018 with 25% fly ash and further dropped to 0.002—indicating non-swelling behaviour—with 25% alkali-activated fly ash. The observed reduction in swelling potential may be attributed to the replacement of clay particles with non-expansive, silt-sized fly ash particles [66–70]. As fly ash is non-plastic, it does not absorb moisture, thus limiting water-induced volume change. Additionally, the formation of NASH during geopolymerisation consumes water, potentially reducing swelling. Turan et al. [4] also observed a reduction in the plasticity index of clay when fly ash was added, noting that lower plasticity correlates with reduced swelling. Further, Phanikumar and Sharma [68] explained that oxides such as silicate, aluminium, and iron in fly ash promote flocculation through cation exchange, leading to increased particle aggregation and reduced swelling. Kolay and Ramesh [63] similarly highlighted the pozzolanic reactivity of fly ash in mitigating swelling in expansive soils. The time-dependent nature of pozzolanic reactions, particularly under prolonged curing, may also contribute to the continuous decline in  $C_s$  values [62, 70, 72].

In this study, the permeability coefficient ( $k$ ) of the soil specimens was determined using the consolidation parameters  $c_v$ ,  $m_v$ , and  $\gamma_w$ , as presented in Whitlow [73],  $\gamma_w$  represents the unit weight of water and  $c_v$  denotes the coefficient of consolidation. The coefficient  $c_v$  was evaluated using Taylor's square root of time method.

Figure 2 shows the permeability results for both untreated and stabilised soil samples across various curing durations. At 1 day of curing, permeability increased with higher contents of fly ash or alkali-activated fly ash. This observation aligns with Mir and Sridharan [62], who also reported elevated permeability values for fly ash-treated soils in the

**Table 2** Influence of fly ash and alkali-activated fly ash dosages and curing duration on compression and swelling indices

Fly ash content (%)	Curing days	Compression index ( $C_c$ )	Swelling index ( $C_s$ )
0% (control sample)	1	0.314	0.053
0% (control sample)	7	0.312	0.051
0% (control sample)	28	0.314	0.048
15% F	1	0.316	0.048
15% F	7	0.229	0.030
15% F	28	0.139	0.030
25%F	1	0.242	0.031
25%F	7	0.190	0.022
25%F	28	0.124	0.018
15% F + AA	1	0.295	0.040
15% F + AA	7	0.132	0.025
15% F + AA	28	0.097	0.012
25% F + AA	1	0.201	0.024
25% F + AA	7	0.106	0.014
25% F + AA	28	0.024	0.002

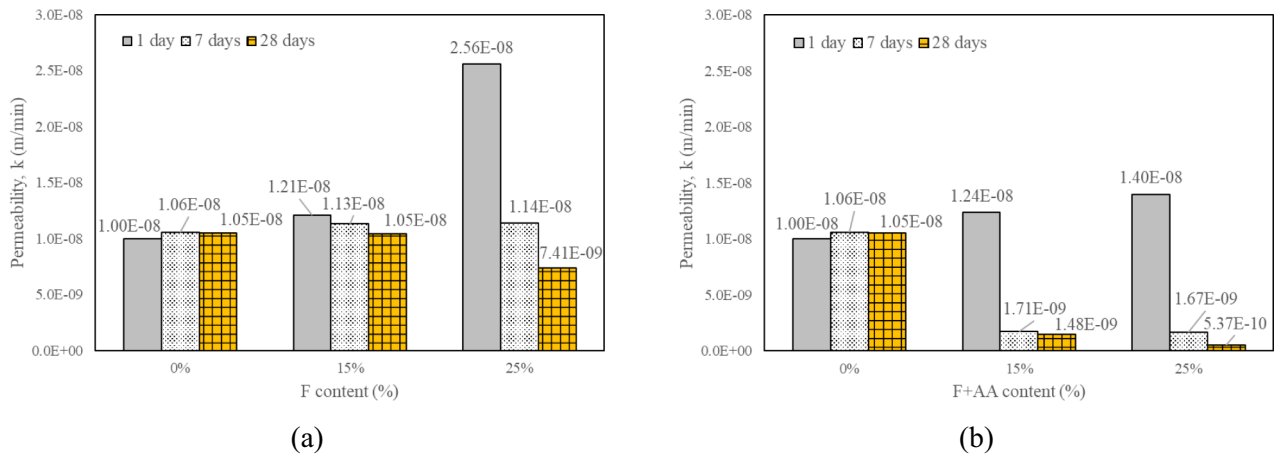


**Fig. 2** Influence of (a) fly ash and (b) alkali-activated fly ash content and curing duration on soil permeability

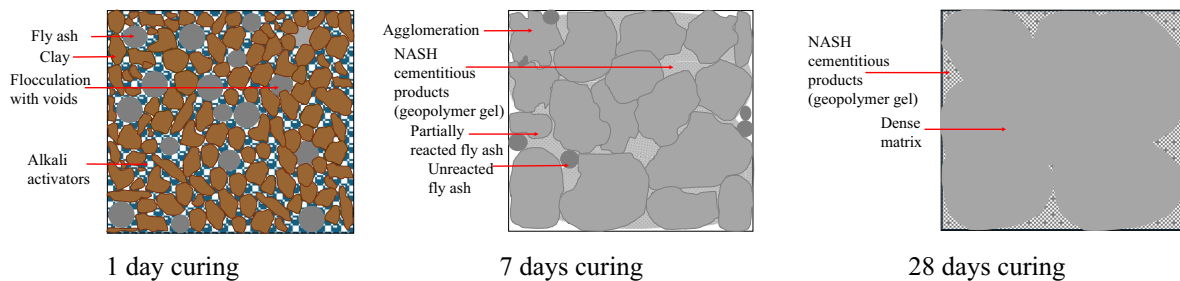
early curing stage, attributing the rise to the incorporation of non-plastic silt-sized particles that enhance soil granularity. Similarly, Phanikumar [61] noted that cation exchange-induced flocculation can lead to increased permeability. However, as curing time progressed, a noticeable decline in permeability was observed, likely due to the formation of cementitious gels during the pozzolanic reaction. These gels gradually fill the pore spaces within the soil matrix, thereby reducing its permeability [74]. As illustrated in Fig. 3, the early stages of geopolymerisation exhibit a relatively open and dispersed structure, associated with the presence of silt particles and incomplete reaction. With time, the structure transitions into a denser matrix through particle agglomeration, leading to a reduction in permeability.

The findings indicated that, at early curing stages, stabilised soils exhibited higher permeability than the untreated control specimens. This increased permeability likely facilitated more efficient pore water drainage during primary consolidation, as also reported by Jaditager and Sivakugan [65]. However, with extended curing, a significant reduction in permeability was observed. Kassim and Chow [74] documented a similar pattern in lime-stabilised soils, noting that elevated permeability at early ages, coupled with increased

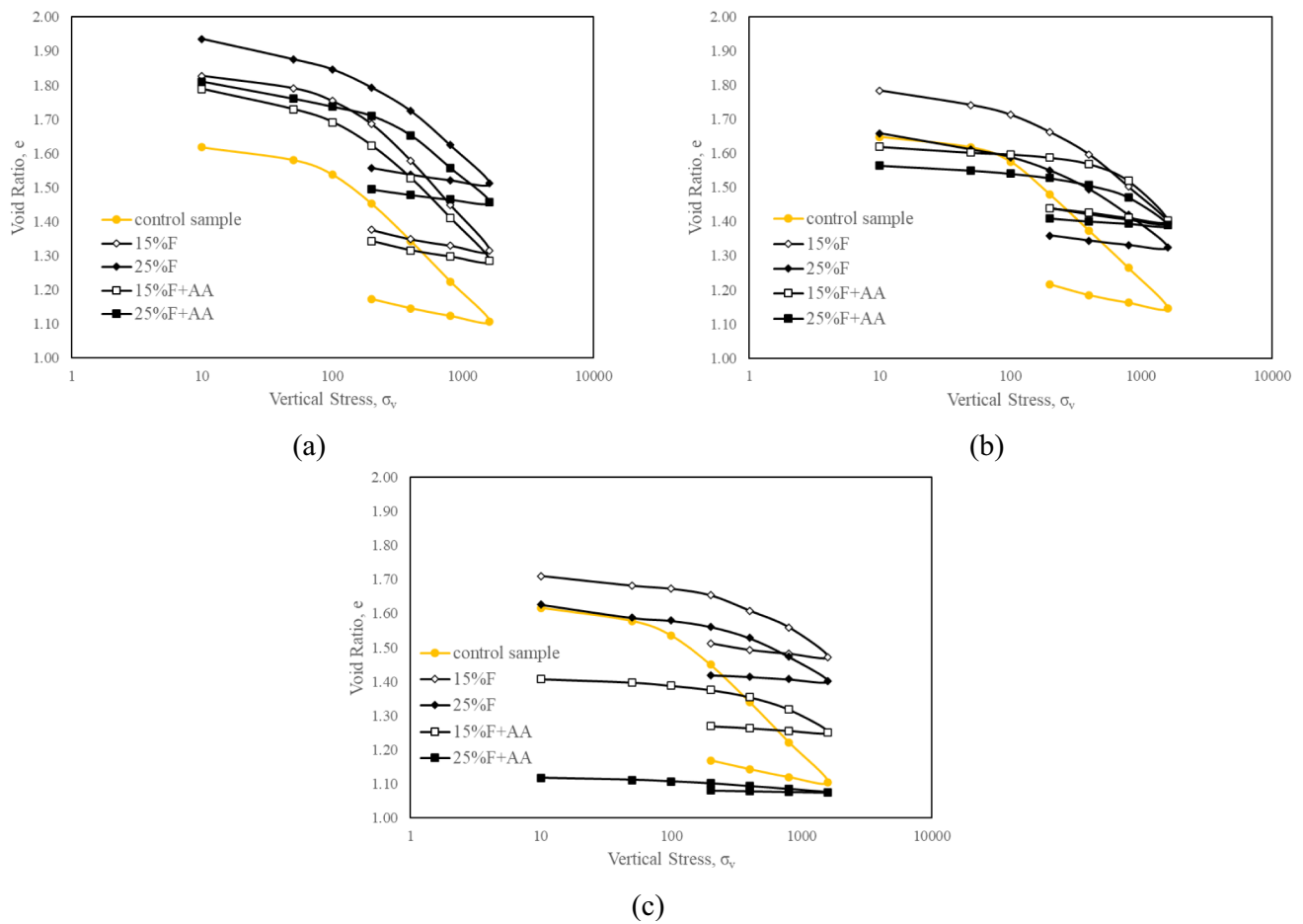
soil stiffness over time, could offer practical advantages in engineering applications.

Figure 4a, b and c shows the  $e-\log \sigma_v$  relationships for the control specimen, fly ash-stabilised soil, and alkali-activated fly ash-stabilised soil at curing periods of 1, 7, and 28 days, respectively. The data reveal that the pre-consolidation pressure, or yield stress, increased with both the inclusion of fly ash or alkali-activated fly ash and with longer curing durations. Notably, the use of alkali-activated fly ash resulted in a more pronounced improvement in yield stress compared to the use of untreated fly ash alone. This enhancement may be attributed to the formation of NASH cementitious bonds between the activated fly ash and clay particles, leading to structural development within the soil matrix. Similar outcomes have been reported in studies involving cement-stabilised clays, where one-dimensional consolidation tests demonstrated that cementation significantly enhances yield stress [75–78].

Curing time had a pronounced affect on the performance of soils treated with alkali-activated fly ash. As indicated in Fig. 5, for samples stabilised with 25% alkali-activated fly ash, the yield stress increased significantly with curing duration—reaching approximately 300 kPa at 1 day, 900 kPa



**Fig. 3** Schematic mechanism of geopolymerisation in clay stabilised with alkali-activated fly ash during curing



**Fig. 4** Effect of fly ash and alkali-activated fly ash content on yield stress at (a) 1 day, (b) 7 days, and (c) 28 days of curing

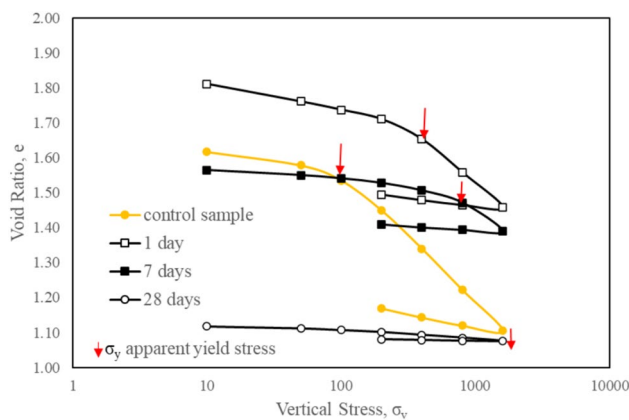


**Fig. 5** Influence of curing duration on yield stress of soil stabilised with 25% alkali-activated fly ash

at 7 days, and exceeding 1100 kPa at 28 days. These results support the notion that time-dependent pozzolanic reactions significantly contribute to the development of strength in the stabilised soil.

Figure 4 demonstrates that, at 1 day of curing, the void ratio of the stabilised soils increased with the addition of fly ash or alkali-activated fly ash, which is typically associated with greater porosity in the soil matrix. This observation aligns with the permeability trends discussed earlier. Similar findings were reported by Jaditager and Sivakugan [65], who attributed the elevated void ratio at early curing stages to the flocculated structure formed as a result of alkali activation in fly ash-based geopolymer-treated soils. As curing progressed, the pozzolanic reaction intensified, leading to the formation of NASH cementitious compounds, which subsequently reduced the void ratio. Despite this reduction, fly ash-stabilised samples maintained a higher void ratio than the untreated control, likely due to the relatively limited cementing capacity of class F fly ash [79]. While its pozzolanic activity contributed modestly to matrix densification, the effect was less significant than that observed with alkali-activated systems. For soils treated with alkali-activated fly ash, the void ratio was initially higher than the control sample at 1 day, but dropped below the control at both 7 and 28 days of curing. This suggests that the development

of NASH gels plays a key role in void filling and structural integration. While Kamruzzaman et al. [77] reported that the reduction in void ratio in cement-treated clay soils was suggested to result from water consumption through hydration and pozzolanic reactions, the continued decrease observed in this study may be attributed to water consumption during NASH gel formation and pozzolanic reactions. This reduction is therefore attributed not only to mechanical consolidation but also to chemical binding of water within the developing geopolymer matrix.

In summary, for the fly ash-treated samples, the void ratio—and by extension, the porosity—remained higher than that of the control even after 28 days of curing. However, these samples still exhibited improved mechanical properties, likely due to the partial pozzolanic reaction contributing to internal bonding and structural enhancement. In contrast, for soils stabilised with alkali-activated fly ash, the initial void ratio was higher than that of the control at 1 day, but decreased significantly by 7 and 28 days as a result of NASH gel formation. In both cases, the observed improvements in

strength and stiffness, despite relatively higher void ratios, suggest that pore connectivity and spatial distribution play a more critical role in mechanical performance than the total pore volume. As hydration and geopolymerisation progress, these processes reduce pore connectivity and promote matrix densification, thereby lowering permeability and enhancing structural integration.

**Triaxial Tests**

*Effect of Curing Duration on Maximum Deviator Stress*

Figure 6a, b and c shows the influence of curing time (1, 7, and 28 days) on the maximum deviator stress ( $q_{max}$ ) of control sample, soils stabilised with 15% and 25% fly ash and alkali-activated fly ash, under effective confining pressures ( $\sigma'_c$ ) of 200, 400, and 600 kPa, respectively. An increasing trend in  $q_{max}$  was observed with longer curing durations, particularly in samples treated with alkali-activated fly ash. These results are consistent with the findings of

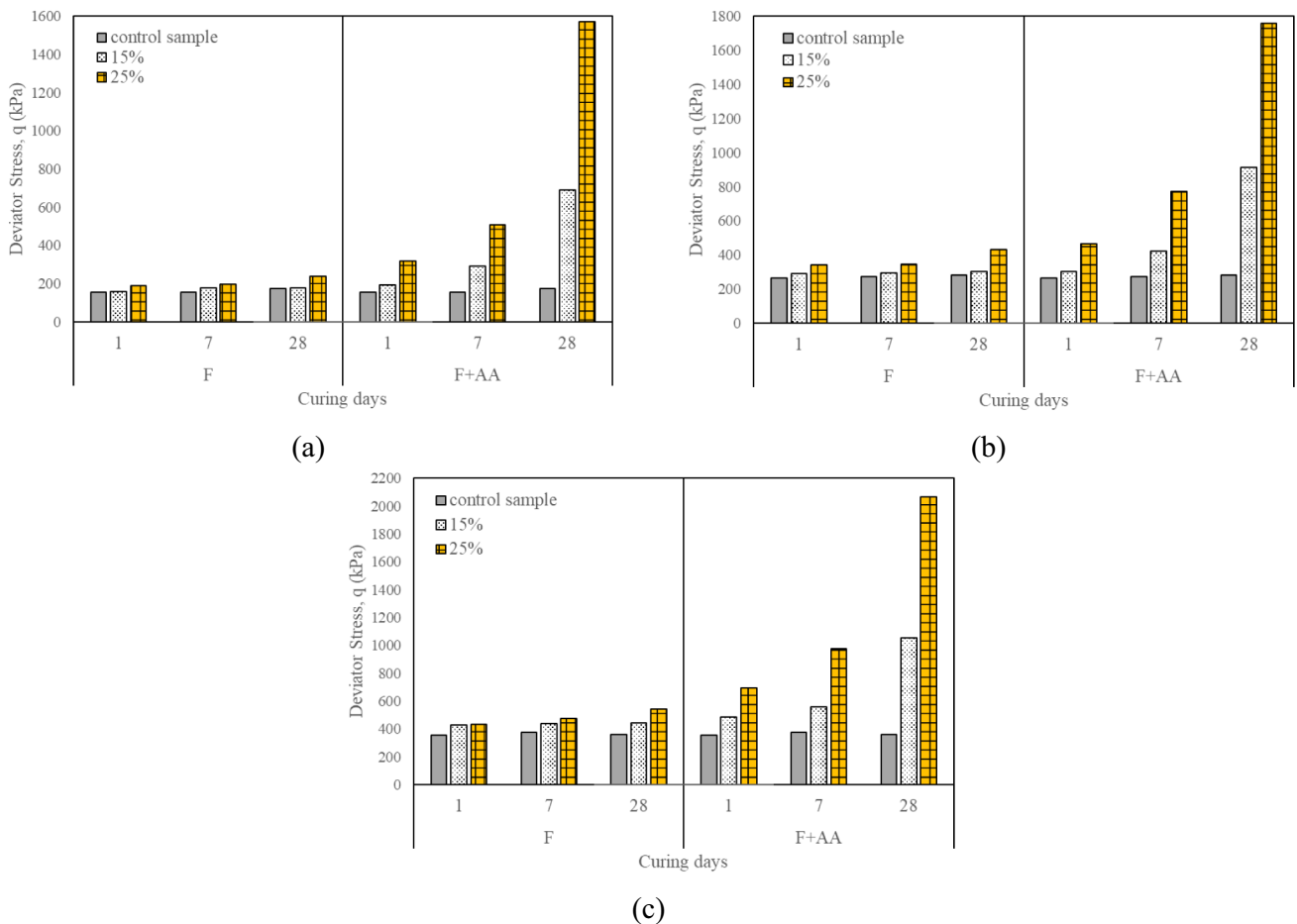


**Fig. 6** Effect of curing duration on maximum deviator stress ( $q_{max}$ ) of control soil and soils stabilised with 15% and 25% fly ash and alkali-activated fly ash under (a) 200 kPa, (b) 400 kPa, and (c) 600 kPa effective confining pressures ( $\sigma'_c$ )

Abdullah et al. [8]. Essentially, the strength gain between 7 and 28 days was more significant than that observed between 1 and 7 days across all confining pressures. This supports observations by Sukmak et al. [28], who emphasised that extended curing periods at ambient temperatures are essential to achieving high strength. Parhi et al. [7] further explained that sufficient time is required not only for the reaction to initiate but also for the accumulation of reaction products derived from the dissolution of aluminosilicate minerals. For example, under a confining pressure of 200 kPa, control specimens exhibited  $q_{\max}$  values of 154, 156, and 176 kPa at 1, 7, and 28 days of curing, respectively, showing negligible change in the absence of pozzolanic activity. In contrast, the inclusion of 15% and 25% alkali-activated fly ash resulted in substantial strength gains: 194 and 319 kPa at 1 day, 292 and 510 kPa at 7 days, and 690 and 1569 kPa at 28 days, respectively. At 28 days, the soil treated with 25% alkali-activated fly ash exhibited a nearly ninefold increase in  $q_{\max}$  compared to the untreated control, highlighting the effectiveness of the stabilisation process.

The results further confirm that  $q_{\max}$  increased with both curing time and fly ash content under confining pressures of 200, 400, and 600 kPa. This trend is consistent with findings by Prabakar et al. [67] and Bryson et al. [80]. However, in the case of fly ash-treated soils without alkali activation, the increase in deviator stress due to curing time alone was minimal. This limited improvement can be attributed to the low-calcium content (2.2%) of class F fly ash, which results in relatively weak cementitious activity at room temperature [79]. Consequently, its chemical interaction with the soil progresses slowly under ambient conditions. The slight enhancement in  $q_{\max}$  for fly ash-stabilised soils may largely stem from changes in soil gradation rather than substantial pozzolanic reactions. Among the tested samples, the highest  $q_{\max}$  values were recorded in soils treated with 25% fly ash after 28 days of curing, across all confining pressure levels. For instance, under a 200 kPa effective confining pressure, the deviator stress increased from 191 to 238 kPa with 25% fly ash, and from 158 to 180 kPa with 15% fly ash over the same curing period. These findings underscore that the inclusion of alkali activators significantly enhances the strength development in fly ash-stabilised soils as curing time progresses.

#### *Stress–Strain Response of Soils Treated with Fly Ash and Alkali-Activated Fly Ash*

Figure 7a, b, c, d, e and f presents the deviator stress ( $q$ )–axial strain ( $\epsilon_a$ ) and excess pore water pressure ( $\Delta_u$ )–axial strain ( $\epsilon_a$ ) relationships for the control sample, soils stabilised with 15% and 25% fly ash and alkali-activated fly ash, following 28 days of curing under effective confining pressures of 200, 400, and 600 kPa.

Figure 7a demonstrates that the control soil exhibited a ductile stress–strain response under effective confining pressures of 200 and 400 kPa, while a slight strain-softening behaviour was observed at 600 kPa. With the incorporation of 15% alkali-activated fly ash, the behaviour transitioned to a brittle, strain-softening response under all confining pressures, as shown in Fig. 7c. The notable increase in maximum deviator stress across all confining pressures is attributed to the geopolymerisation process triggered by alkali activation. The use of 25% alkali-activated fly ash further intensified this response, producing a more sudden post-peak softening with increased initial stiffness, indicated by a steeper pre-peak slope and higher stress peak [80]. Additionally, the axial strain corresponding to  $q_{\max}$  decreased significantly with alkali-activated fly ash. At 28 days of curing, the control sample reached  $q_{\max}$  values of 176, 283, and 359 kPa under 200, 400, and 600 kPa confining pressures, respectively, at axial strains of approximately 17%, 20%, and 11%. In contrast, soils treated with 25% alkali-activated fly ash achieved much higher  $q_{\max}$  values of 1569, 1761, and 2067 kPa at significantly lower axial strains of 1.1%, 1.0%, and 0.9%, respectively. Similar trends were observed by Abdullah et al. [8] in their study of geopolymer-stabilised soils, where the increased undrained strength was attributed to the formation of strong geopolymeric bonds during the pre-yield phase. Once shearing commenced, these bonds failed, and the post-yield behaviour became governed by frictional resistance within a weakened, destructured soil matrix. Kamruzzaman et al. [77] also observed comparable patterns in cement-stabilised soils, where higher cement contents led to more pronounced strain-softening due to greater bond destructure. They noted that when the strength of cementitious bonds is sufficiently high, the mechanical behaviour of the stabilised soil resembles that of overconsolidated structured natural clays, particularly when the effective confining pressure is lower than the yield stress. In contrast, soils stabilised with 15% and 25% class F fly ash without alkali activation maintained a ductile stress–strain profile similar to the control sample (Fig. 7e). Only marginal increases in  $q_{\max}$  were observed with increasing fly ash content under all confining pressures.

The deviator stresses of control sample, soils stabilised with alkali-activated fly ash and soils stabilised with fly ash, all showed increase with the increase in confining pressure (Fig. 7a, c and e). This is because, the higher the confining pressure, the higher the change in fabric during consolidation stage. Consequently, higher volume change can be observed, therefore  $q_{\max}$  of soil sample increase [75, 77]. However, this condition is more obvious when the effective confining pressure of the sample is higher than the yield stress (i.e. soil is normally consolidated); this is due to the higher effect of reorientation in clay matrix during consolidation stage. The  $q_{\max}$  rate of control sample from 200 to

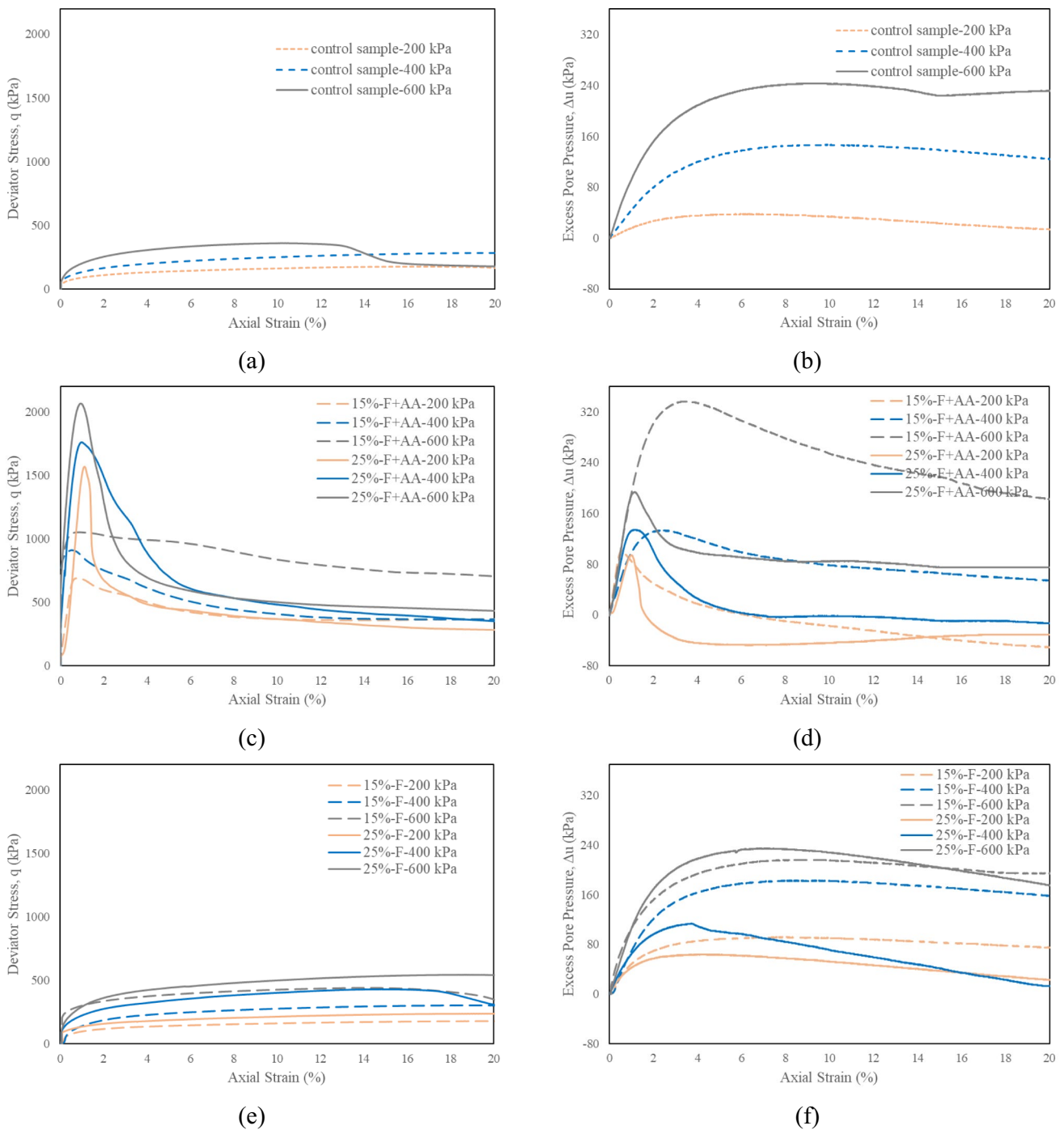


**Fig. 7** Stress–strain and pore pressure–strain behaviour under 200, 400, and 600 kPa confining pressures after 28 days of curing. **(a, b)** control sample, **(c, d)** soils stabilised with 15% and 25% F+AA, **(e, f)** soils stabilised with 15% and 25% F

400 kPa  $\sigma'_c$  was 1.7, while the rate of soils stabilised with 25% of alkali-activated fly ash showed 1.1 under the same  $\sigma'_c$  (Fig. 7a, c). This indicates that the yield stress of soils with alkali-activated fly ash is much higher than the control sample.

As shown in Fig. 7b, d and f, the excess pore pressure–axial strain responses closely reflect the corresponding

stress–strain behaviour across all tested samples. For the control specimen, positive excess pore pressures were observed under all confining pressures. These samples typically reached peak pore pressure at axial strains between 6 and 10%, followed by a slight reduction under effective confining pressures of 200, 400, and 600 kPa (Fig. 7b). A similar trend was also observed in soils stabilised with fly

ash, where peak pore pressures occurred at comparable strain levels before exhibiting a gradual decline (Fig. 7f). In contrast, soils stabilised with 15% and 25% alkali-activated fly ash (Fig. 7d) exhibited pore pressure curves that initially increased to a peak at small strain levels, then decreased sharply and stabilised at a constant value—demonstrating a classic strain-softening response. A higher content of alkali-activated fly ash resulted in a lower axial strain at the peak. For instance, the axial strain at peak pore pressure in soils treated with 25% alkali-activated fly ash remained around 1% under confining pressures of 200, 400, and 600 kPa, whereas both the control sample and the soil treated with 25% fly ash exhibited peak strains ranging between approximately 6% and 8% under the same effective confining pressures. At low confining pressures and higher alkali-activated fly ash content, the volume change behaviour shifted from contractive to dilative. Under undrained shear conditions, where drainage is not allowed, this dilation led to the development of negative excess pore pressures, similar to the behaviour of heavily overconsolidated clays. This response was evident in soils treated with 15% alkali-activated fly ash at 200 kPa, and with 25% at both 200 and 400 kPa. This transition from contractive to dilative behaviour has also been reported by Abdullah et al. [8], who noted similar negative pore pressure development in clay soils treated with fly ash and slag under low  $\sigma'_c$  conditions. The development of negative excess pore pressures in alkali-activated fly ash-stabilised soils can be attributed to the formation of a rigid interparticle structure through NASH gel networks, which promote dilative behaviour under undrained shear. Meanwhile, the excess pore pressure responses of soils stabilised with 15% and 25% class F fly ash (Fig. 7f) resembled those of the control sample, showing no indication of overconsolidated behaviour, even under low confining pressures. This can be attributed to the low cementitious potential of class F fly ash, which limits bond formation necessary for such behaviour to manifest. An increase in effective confining pressure was associated with higher excess pore water pressures across all tested samples, as shown in Fig. 7b, d and f. This trend is consistent with findings from previous studies on cement-stabilised soils [e.g. 75, 77, 81, 82]. According to Luis et al. [82], as  $\sigma'_c$  increases, the applied stress can compromise the integrity of cementitious bonds, thereby accelerating the stabilisation of excess pore pressure under higher confining stress levels.

#### *Shear Strength Characteristics of Soils Treated with Fly Ash and Alkali-Activated Fly Ash*

Mohr–Coulomb shear strength parameters were derived from consolidated-undrained (CU) triaxial tests conducted under three levels of effective confining pressure to evaluate the effective cohesion ( $c'$ ) and effective angle of shearing

resistance ( $\phi'$ ) of the control soil, soils stabilised with fly ash and alkali-activated fly ash, at curing periods of 1, 7, and 28 days, as summarised in Table 3.

The results indicate that the effective cohesion ( $c'$ ) of soils treated with alkali-activated fly ash increased with both higher fly ash content and longer curing durations. This enhancement in  $c'$  can be attributed to the greater formation of geopolymeric products and improved bonding between soil particles as the fly ash dosage increases. Correa-Silva et al. [29, 83] noted that alkaline binders significantly influence shear strength by acting as a glue-like medium, promoting interparticle bonding and strengthening the cementitious structure. Horpibulsuk et al. [75] also highlighted that a higher degree of cementitious bonding corresponds to increased cohesion. Moreover, the increase in  $c'$  was more pronounced at later curing ages. According to Turan et al. [54], the reaction between sodium silicate (SS), sodium hydroxide (SH), and fly ash generates time-dependent NASH compounds, enhancing particle bonding over time. Similarly, Correa-Silva et al. [83] reported progressive development of reaction products in alkali-activated soils, resulting in continued improvement in  $c'$  between 28 and 90 days of curing. In contrast, soils stabilised with class F fly ash exhibited lower  $c'$  values compared to the control sample across all curing times. This outcome is primarily due to the low-calcium content and silty nature of class F fly ash, which limits its reactivity [79], as also reported by Rajak et al. [84]. Nevertheless, a slight increase in  $c'$  was observed over time, likely due to the pozzolanic activity of the fly ash contributing gradually to bonding within the soil matrix.

**Table 3** Effective cohesion and angle of shearing resistance of control soil and soils stabilised with 15% and 25% fly ash and alkali-activated fly ash at various curing periods

Fly ash content (%)	Curing days	$c'$ (kPa)	$\phi'$ (°)
0%	1	17.5	18.1
0%	7	18.5	19.6
0%	28	19.0	18.4
15% F+AA	1	17.6	21.3
15% F+AA	7	43.7	22.2
15% F+AA	28	183.3	22.6
25% F+AA	1	26.3	25.7
25% F+AA	7	101.8	27.0
25% F+AA	28	388.6	29.0
15% F	1	2.7	20.7
15% F	7	4.9	21.1
15% F	28	11.1	22.3
25% F	1	8.4	21.6
25% F	7	10.1	21.6
25% F	28	15.1	22.4

To better emphasise the increase in cohesion resulting from the bonding mechanism, a limited microstructural investigation using SEM analysis was conducted on the control sample, soils stabilised with 25% alkali-activated fly ash and 25% untreated fly ash after a 28 day curing period, as shown in Fig. 8a, b, and c (100 and 10  $\mu\text{m}$ ), respectively. Figure 8a shows that the kaolinite consists of platy-shaped clay particles and exhibits a relatively less permeable microstructure. The overall morphology also reveals a uniform and orderly microstructural arrangement typical of untreated clay. In Fig. 8b, the presence of NASH cementitious products is observed, along with the filling of voids by these gels over time, thereby enhancing interlocking structures and ultimately leading to the formation of a dense matrix after 28 days. The more compact structure may contribute to increased strength and stiffness in the stabilised soil [85, 86], also indicating greater cohesion. The disappearance of spherical fly ash particles after 28 days in soils stabilised with alkali-activated fly ash is primarily attributed to the leaching of aluminosilicate materials from the fly ash under highly alkaline conditions. This leaching process induces particle dissolution, ultimately resulting in the loss of their spherical morphology [13]. On the other hand, Fig. 8c shows that, despite the 28 day curing period, unreacted fly ash particles, pores, and clay particles remain distinctly visible in soils stabilised with untreated fly ash. Nevertheless, a limited amount of pozzolanic reaction products is observed which explains the minor increase in cohesion noted earlier. In general, the dense matrix formed in soils stabilised with alkali-activated fly ash and the lack of a well-developed bonding structure in soils stabilised with fly ash are consistent with the cohesion results presented in Fig. 8a, b and c.

The effective angle of shearing resistance ( $\varphi'$ ) was consistently higher in soils stabilised with both fly ash and alkali-activated fly ash compared to the control sample across all curing durations. Specifically, the inclusion of 25% alkali-activated fly ash increased  $\varphi'$  from 18.4° in the control sample to 29° after 28 days of curing, whereas a similar dosage of untreated fly ash resulted in a  $\varphi'$  value of 22.4° at the same curing age. Previous studies have linked this increase in  $\varphi'$  primarily to particle substitution mechanisms [79, 80, 84]. The presence of silt-sized particles in fly ash reduces the proportion of clay in the soil matrix, thereby increasing the average grain size and enhancing frictional resistance [80]. Furthermore, soils treated with alkali-activated fly ash exhibited higher  $\varphi'$  values than those treated with fly ash alone. According to Horpibulsuk et al. [75], cementitious reaction products act as a binding agent, reinforcing the soil matrix and enabling greater resistance to distortion during shearing. This structural reinforcement contributes not only to improved cohesion but also to a higher angle of internal friction. Additionally, a clear trend of increasing  $\varphi'$  with curing time was observed, likely due to the progressive

development of cementitious bonds and pozzolanic reactions. Sezer et al. [87] also noted that moisture loss over time may contribute to increased shearing resistance, further supporting this trend.

#### *Critical State Parameters of Soils Treated with Fly Ash and Alkali-Activated Fly Ash*

Consolidated-undrained (CU) triaxial tests were performed under effective confining pressures of 200, 400, and 600 kPa. The resulting critical state lines in the  $q$ - $p'$  plane for the control soil, as well as for soils stabilised with fly ash and alkali-activated fly ash at curing times of 1, 7, and 28 days, are presented in Fig. 9a, b and c. In CU triaxial tests, the critical state line is typically identified within an axial strain range of 15–20%, as commonly adopted in the literature [88, 89]. Considering that stabilised soils incorporating cementitious materials may require larger strains to reach the critical state, a reference axial strain of 20% was adopted in this study. At this strain level, the stabilisation of pore water pressure and stress values was confirmed, indicating that the specimens had reached the critical state. It was observed that the inclusion of either fly ash or alkali-activated fly ash led to an increase in the slope of the critical state line, denoted as  $M$ . Since  $M$  is closely associated with the angle of shearing resistance and reflects the interaction and geometric arrangement of soil particles [90], the improvement in  $M$  is likely due to the silty texture of fly ash, which alters the particle structure of the stabilised soils. Among the stabilised specimens, those treated with alkali-activated fly ash consistently exhibited higher  $M$  values than those treated with fly ash-only across all curing periods. This finding aligns with the trends observed in the previously discussed Mohr–Coulomb shear strength parameters. Similar increases in  $M$  have been reported by Subramaniam et al. [78] for cement-stabilised clays and by Abdullah et al. [8] for clays treated with alkali-activated slag. The increase in  $M$  is believed to be influenced by the formation of larger and stiffer geopolymer-induced bonds, which enhance particle interaction and shear resistance within the soil matrix [8]. Furthermore, the value of  $M$  increased with curing time in all stabilised soils, likely due to the progressive development of cementitious bonds and pozzolanic reaction products. For the stabilised soils, the  $y$ -intercept of the critical state line in  $q$ - $p'$  plane increased with the increase in alkali-activated fly ash and the curing times. The increase in the  $y$ -intercept in the stabilised soils can be attributed to the effects of cementation bonding [90]. In the soils stabilised with alkali-activated fly ash, cementation occurred during the geopolymerisation process [8]. A similar development was observed by Robin et al. [90] who run triaxial tests on soils stabilised with lime. On the other hand, the  $y$ -intercept of the critical state line (CSL) for the

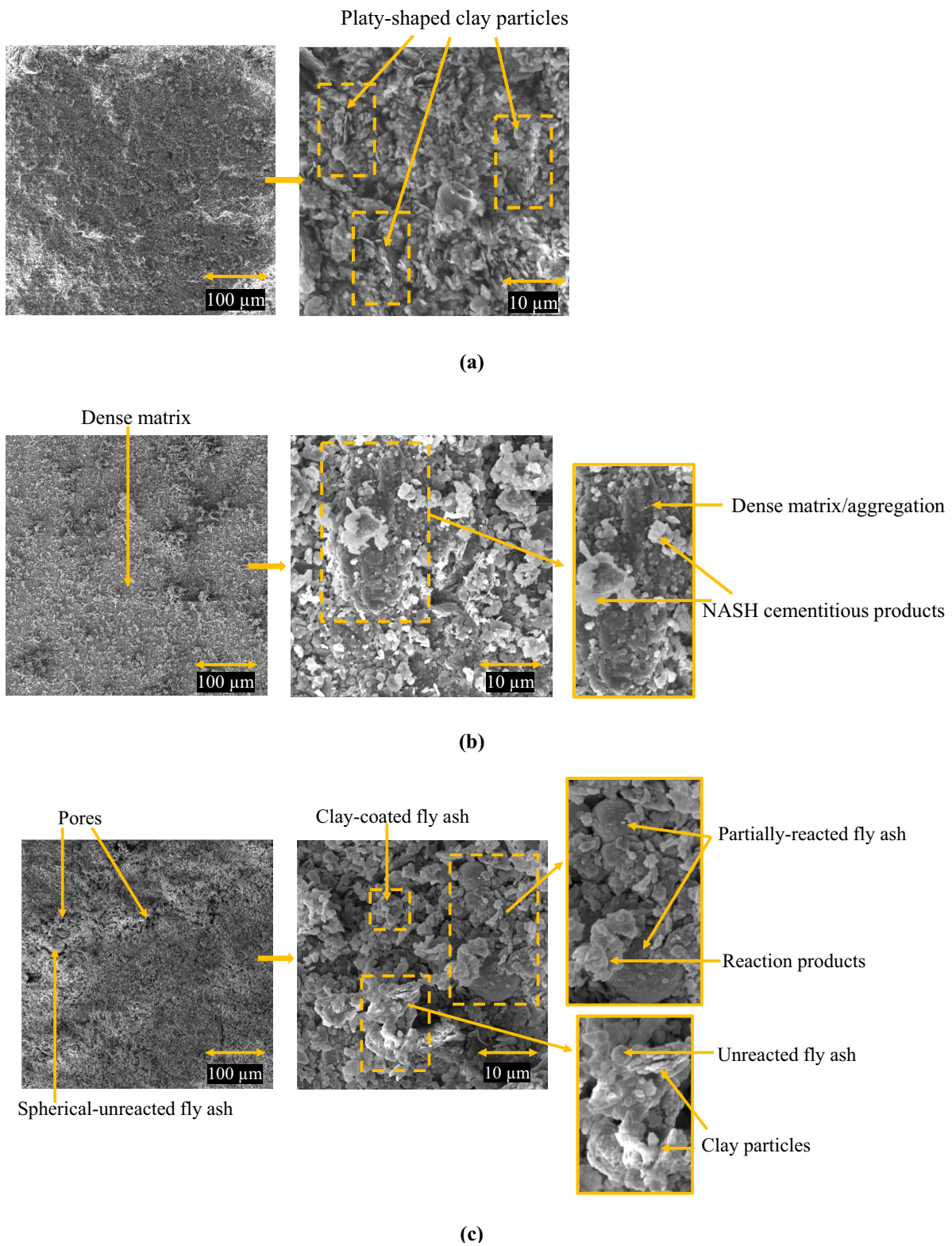


**Fig. 8** SEM micrographs at 100 μm and 10 μm scales for: (a) control sample (kaolinite), (b) clay treated with alkali-activated fly ash, and (c) clay treated with class F fly ash after 28 days of curing

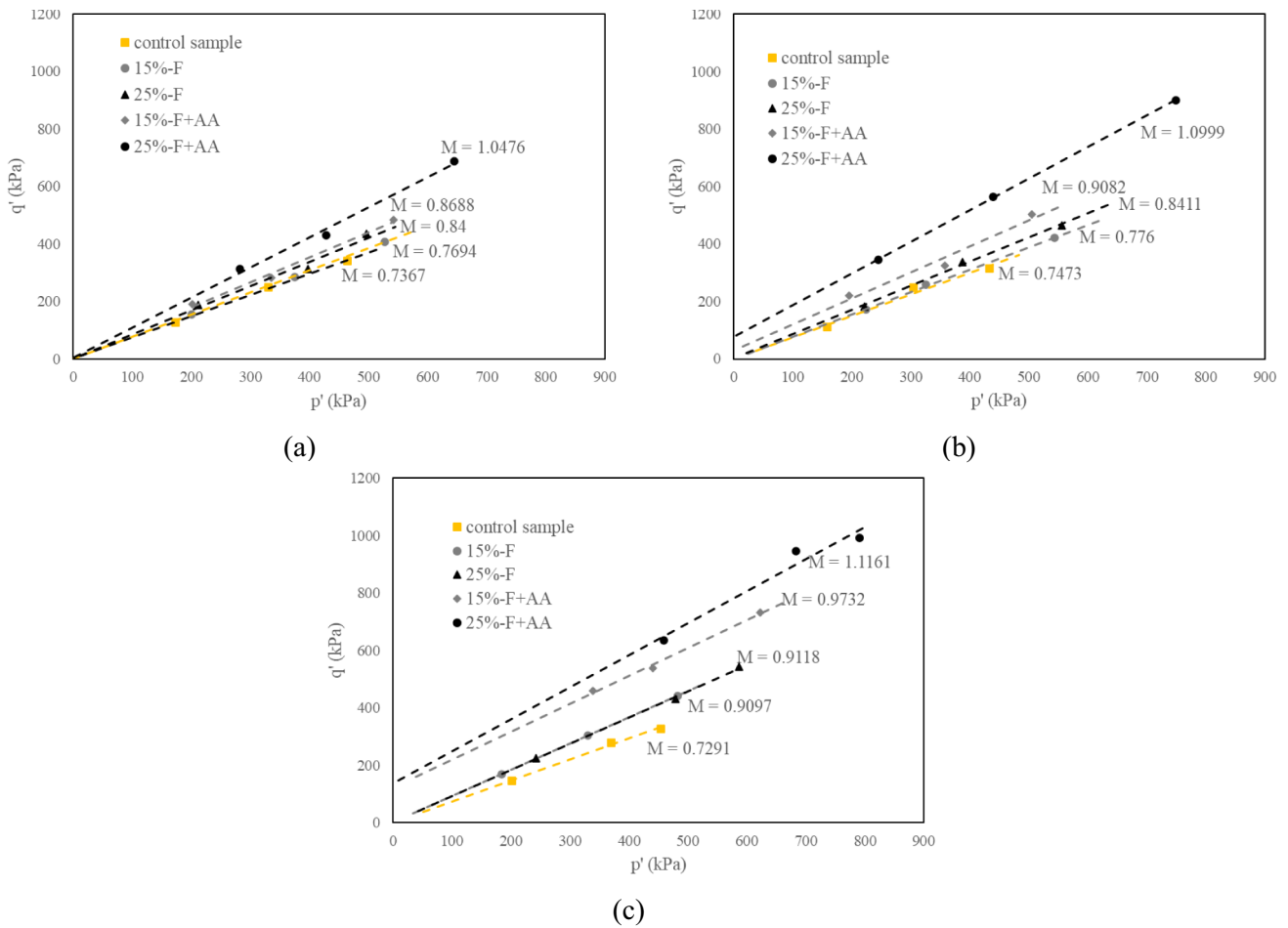


**Fig. 9** Critical state lines in the  $q$ - $p'$  plane for control soil and soils stabilised with fly ash and alkali-activated fly ash at (a) 1 day, (b) 7 days, and (c) 28 days of curing

soils stabilised with class F fly ash in  $q'$ - $p'$  plane was stable due to the low-calcium amount and thus low cementation.

Figure 10a, b and c presents the critical state lines in the  $v$ - $\ln p'$  space for the control soil and for samples treated with class F fly ash and alkali-activated fly ash after 1, 7, and 28 days of curing, respectively. As confirmed by the  $q$ - $p'$  plots for each CU triaxial test, the void ratio ( $e$ ) was calculated at 20% axial strain using the corresponding water content and the known specific gravity of solids ( $G_s$ ). The specific volume was then determined as  $v = 1 + e$ . Together with the natural logarithm of the mean effective stress at the same strain level, the  $(v, \ln p')$  coordinates were identified to define the critical state line, in accordance with the methodology described by Fonseca et al. [89]. The critical state parameters  $\lambda$  and  $\Gamma$  were determined using the following equation:

$$v = \Gamma - \lambda \ln(p') \tag{1}$$

In the critical state framework,  $\Gamma$  represents the specific volume on the CSL at  $p' = 1$  kPa, while  $\lambda$  denotes the slope of the CSL. The parameter  $\lambda$  is also associated with the compression index ( $C_c$ ), which characterises the consolidation and settlement behaviour of soils [91]. Based on the experimental results, both  $\lambda$  and  $\Gamma$  decreased with increasing alkali-activated fly ash content at all curing stages, and with increasing fly ash content at 7 and 28 days of curing. A similar trend was reported by Kichou [92], who observed reduced compressibility in London clay stabilised with lime through triaxial testing. These findings suggest that the compressibility of soils treated with 15% and 25% alkali-activated fly ash or fly ash was effectively reduced. This outcome is consistent with the observations made by Phanikumar and Sharma [68], Kolay and Ramesh [71], and Bryson et al. [80]. However, in the case of soils stabilised with 15% and 25% class F fly ash at 1 day of curing, the  $\Gamma$  value initially increased compared to the control sample, followed by a reduction at 7 and 28 days. Phanikumar [61] and Bryson et al. [80]

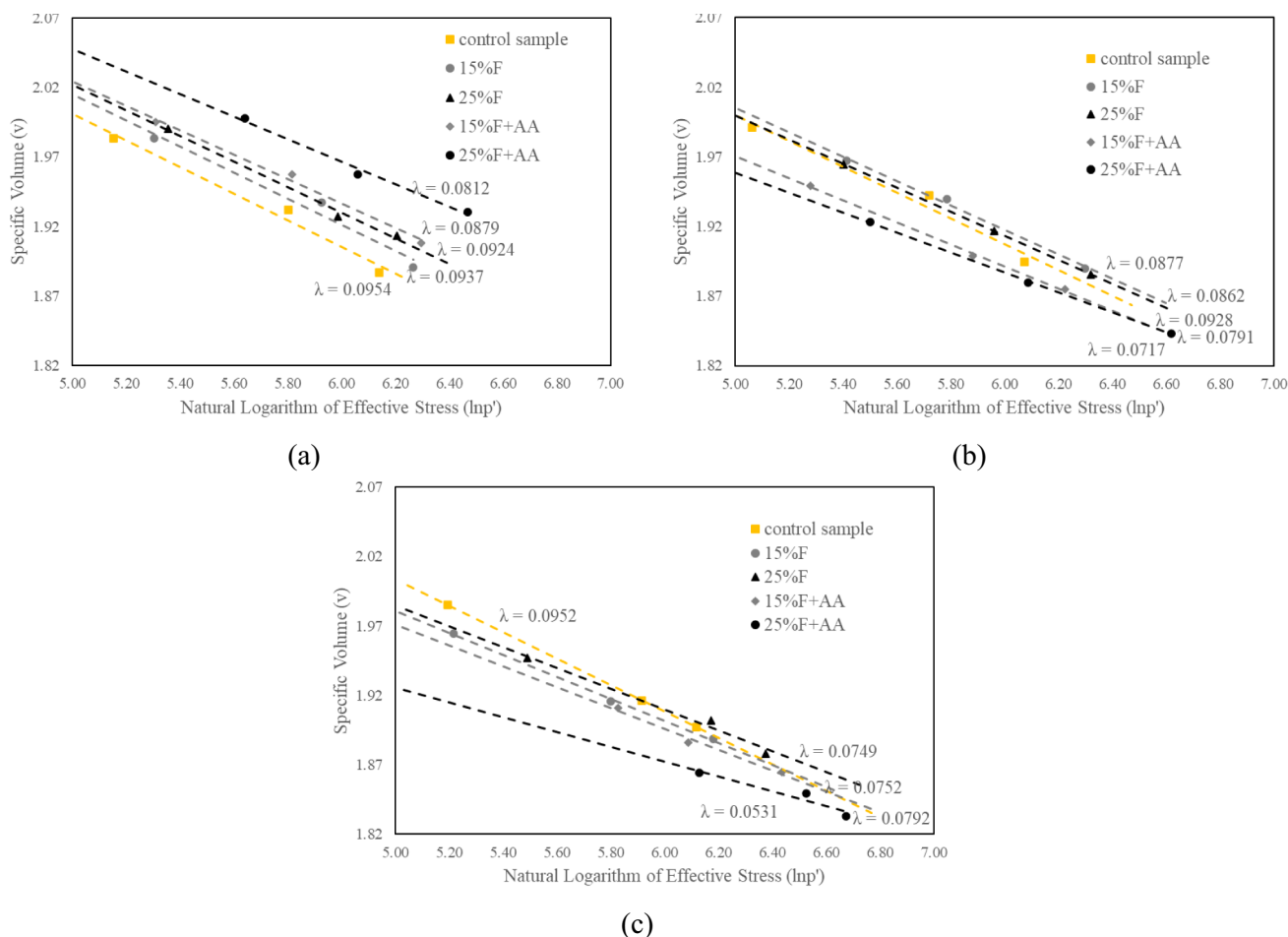


**Fig. 10** Critical state lines in the  $v\text{-}lnp'$  plane for control soil and soils stabilised with fly ash and alkali-activated fly ash at (a) 1 day, (b) 7 days, and (c) 28 days of curing

similarly reported that the compression index tends to increase at early curing stages with higher class F fly ash content, likely due to its limited cementitious reactivity. These results indicate that curing time is a critical factor in improving the compressibility behaviour of soils treated with class F fly ash.

At 28 days of curing, the  $\Gamma$  value for the control sample was 2.48. This value decreased to 2.35 and 2.19 for soils stabilised with 15% and 25% alkali-activated fly ash, respectively. For soils treated with 15% and 25% class F fly ash, the corresponding  $\Gamma$  values were slightly reduced to 2.38 and 2.36. Similarly, the  $\lambda$  value for the control sample was recorded as 0.095, which dropped to 0.075 and 0.053 for the alkali-activated fly ash-stabilised soils, and to 0.079 and 0.075 for those stabilised with class F fly ash. These findings clearly demonstrate the notable influence of alkali activators in reducing the compressibility characteristics of the stabilised soils.

### Conclusions

This study evaluated the factors affecting the geomechanical properties of clay stabilised with alkali-activated fly ash and class F fly ash through one-dimensional consolidation and consolidated-undrained triaxial tests. The following conclusions can be drawn from the study:

- The compression index generally decreased with fly ash or alkali-activated fly ash and curing time, except at 1 day where 15% fly ash caused a slight increase before decreasing at 25% dosage. The swelling index decreased with fly ash or alkali-activated fly ash addition and curing time, owing to the non-expansive and pozzolanic nature of fly ash.
- The permeability of the soil stabilised with alkali-activated fly ash was greater than the control sample at early curing times. However, the value of  $k$  decreased as the

time progressed and it became less permeable compared to the control sample. The void ratio of the stabilised soil followed a trend similar to permeability.

- Curing time markedly enhanced deviator stress in soils treated with alkali-activated fly ash, especially between 7 and 28 days, while class F fly ash alone had minimal effect regardless of dosage or curing duration.
- Alkali-activated fly ash altered the stress–strain behaviour from ductile to brittle at 28 days, with 25% content leading to a stiffer and sharper post-peak response. In contrast, fly ash-only samples maintained ductile behaviour. Increasing confining pressure raised both maximum deviator stress and excess pore water pressure in all stabilised soils.
- The addition of alkali-activated fly ash significantly improved the  $c'$  and  $\phi'$  of the stabilised soils, with  $c'$  reaching 388.6 kPa and  $\phi'$  increasing to  $29^\circ$  at 28 days of curing for soils stabilised with 25% alkali-activated fly ash. This improvement is attributed to enhanced geopolymerisation, pozzolanic reactions, and increased cementitious bonding, which were more pronounced in alkali-activated fly ash than in class F fly ash.
- The critical state parameter  $M$  increased with higher alkali-activated fly ash or fly ash content and curing time, while  $\lambda$  and  $\Gamma$  decreased. For class F fly ash,  $\Gamma$  initially rose at 1 day, then declined at later curing stages.

In general, the inclusion of alkali activators with class F fly ash significantly improves the geomechanical properties of stabilised clay compared to using untreated fly ash alone. The chemical activation process induced by alkali activation promotes the formation of additional cementitious compounds, enhancing the strength, stiffness, and consolidation performance of stabilised soils.

### Recommendations for future research

The primary objective of this study is to contribute to the current understanding of the geomechanical behaviour of alkali-activated fly ash-stabilised soils—particularly kaolinitic clays—under controlled laboratory conditions. Future research should address the long-term durability of alkali-activated stabilised soils under varying environmental conditions, particularly cyclic wetting and drying and freeze–thaw cycles. These environmental factors are critical to understanding the resilience and service life of geopolymer-treated soils in field applications.

In particular, it is recommended that future studies incorporate long-term immersion testing to evaluate the effects of sustained saturation. This is especially important for assessing potential strength degradation due to leaching or continuous moisture exposure, which may not be fully captured through short-term or cyclic tests. Such investigations would

provide a more comprehensive understanding of the long-term performance and practical applicability of fly ash and alkali-activated systems in water-sensitive environments.

In addition, comparative studies involving alternative, lower-cost activators (e.g. sodium carbonate) should be conducted to assess their mechanical performance and environmental impact. Further investigations should also focus on field-scale validation and comprehensive cost–benefit analyses to bridge the gap between laboratory-scale performance and real-world implementation.

It should also be noted that the experimental investigation in this study was conducted on a specific type of synthetic clayey soil with controlled properties. Therefore, the findings should be interpreted within the limitations of the tested material. For broader generalisation, future studies are recommended to include a comparative assessment using natural clayey soils with varying mineralogical compositions and plasticity characteristics. Such investigations would help to evaluate the consistency and applicability of the observed behaviour across a wider range of soil types commonly encountered in geotechnical practice.

### Suggested field applications

The results of this study demonstrate that alkali-activated fly ash can significantly improve the strength and compressibility of kaolinitic clays, making it a suitable candidate for stabilising weak cohesive soils in practical applications. For field use, careful material preparation—including pulverisation of clay—and appropriate mixing techniques (dry or wet) should be adopted to ensure uniform treatment. These procedures align with existing practices in road subgrade and embankment construction and could be applied in current geotechnical projects without major changes.

**Funding** No external funding or grants were received for the research presented in this manuscript.

### Declarations

**Conflict of interest** The authors declare no conflict of interest.

### References

1. Munda J, Ram AK, Mohanty S (2023) Small-strain shear modulus and strength characteristics of clayey soil treated with Nano-SiO<sub>2</sub> and fly ash. *Int J Civ Eng* 21:1813–1833. <https://doi.org/10.1007/s40999-023-00857-x>
2. Ghadir P, Ranjbar N (2018) Clayey soil stabilization using geopolymer and Portland cement. *Constr Build Mater* 188:361–371. <https://doi.org/10.1016/j.conbuildmat.2018.07.207>
3. Kandalai S, Patel A (2025) Alkali activation of red mud and ggbs blends for expansive soil stabilization: strength, durability

- and leachate studies. *Indian Geotech J.* <https://doi.org/10.1007/s40098-025-01183-w>
4. Turan C, Javadi A, Vinai R, Cuisinier O, Russo G, Consoli NC (2019) Mechanical properties of calcareous fly ash stabilized soil. *Eurocoalash 1*:184–194
  5. Murmu AL, Dhole N, Patel A (2018) Stabilisation of black cotton soil for subgrade application using fly ash geopolymer. *Road Mater Pavement Des* 21:867–885. <https://doi.org/10.1080/14680629.2018.1530131>
  6. Wong B, Wong K, Phang I (2019) A review on geopolymerisation in soil stabilization. *IOP Conf Ser: Mater Sci Eng* 495:012070. <https://doi.org/10.1088/1757-899x/495/1/012070>
  7. Parhi PS, Garanayak L, Mahamaya M, Das SK (2018) Stabilization of an expansive soil using alkali activated fly ash based geopolymer. In: Hoyos L, McCartney J (eds) *Advances in Characterization and Analysis of Expansive Soils and Rocks*. Springer, Cham, pp 36–50
  8. Abdullah HH, Shahin MA, Walske ML (2019) Geo-mechanical behavior of clay soils stabilized at ambient temperature with fly-ash geopolymer-incorporated granulated slag. *Soils Found* 59:1906–1920. <https://doi.org/10.1016/j.sandf.2019.08.005>
  9. Abdullah HH, Shahin MA, Walske ML, Karrech A (2020) Cyclic behaviour of clay stabilised with fly-ash based geopolymer incorporating ground granulated slag. *Transportation Geotechnics* 26:100430. <https://doi.org/10.1016/j.trgeo.2020.100430>
  10. Behnood A (2018) Soil and clay stabilization with calcium- and non-calcium-based additives: a state-of-the-art review of challenges, approaches and techniques. *Transp Geotech* 17:14–32. <https://doi.org/10.1016/j.trgeo.2018.08.002>
  11. Pacheco-Torgal F, Castro-Gomes J, Jalali S (2007) Alkali-activated binders: a review: part 2. about materials and binders manufacture. *Constr Build Mater* 22:1315–1322. <https://doi.org/10.1016/j.conbuildmat.2007.10.015>
  12. Yaghoubi M, Arulrajah A, Disfani MM, Horpibulsuk S, Darmawan S, Wang J (2019) Impact of field conditions on the strength development of a geopolymer stabilized marine clay. *Appl Clay Sci* 167:33–42. <https://doi.org/10.1016/j.clay.2018.10.005>
  13. Rios S, Cristelo N, da Fonseca AV, Ferreira C (2016) Structural performance of alkali-activated soil ash versus soil cement. *J Mater Civ Eng* 28:04015125. [https://doi.org/10.1061/\(asce\)mt.1943-5533.0001398](https://doi.org/10.1061/(asce)mt.1943-5533.0001398)
  14. Zhuang XY, Chen L, Komarneni S, Zhou CH, Tong DS, Yang HM, Yu WH, Wang H (2016) Fly ash-based geopolymer: clean production, properties and applications. *J Clean Prod* 125:253–267. <https://doi.org/10.1016/j.jclepro.2016.03.019>
  15. Dibamehr A, Sarand FB, Sorkhabi RV (2025) Application of geopolymerization as a new method for stabilizing marl soil. *Indian Geotech J.* <https://doi.org/10.1007/s40098-024-01157-4>
  16. Abdullah MMA, Hussin K, Bnhussain M, Ismail KN, Ibrahim WMW (2011) Mechanism and chemical reaction of fly ash geopolymer cement—a review. *International Journal of Pure and Applied Sciences and Technology* 6:35–44
  17. Phummiphan I, Horpibulsuk S, Sukmak P, Chinkulkijniwat AA, Shen S-L (2016) Stabilisation of marginal lateritic soil using high calcium fly ash-based geopolymer. *Road Mater Pavement Des* 17(4):877–891. <https://doi.org/10.1080/14680629.2015.1132632>
  18. Van Deventer SJSJ, Lukey GC, Xu H (2006) Effect of curing temperature and silicate concentration on fly ash based geopolymerization. *Ind Eng Chem Res* 45:3559–3568
  19. Al Bakri AM, Faheem TM, Sandhu AV, Alida A, Salleh MAAM, Ruzaidi C (2013) Microstructure studies on different types of geopolymer materials. *Appl Mech Mater* 421:384–389. <https://doi.org/10.4028/www.scientific.net/amm.421.384>
  20. van Jaarsveld JGS, van Deventer JSJ, Lukey GC (2003) The characterisation of source materials in fly ash-based geopolymers. *Mater Lett* 57:1272–1280. [https://doi.org/10.1016/s0167-577x\(02\)00971-0](https://doi.org/10.1016/s0167-577x(02)00971-0)
  21. Criado M, Fernandez-Jimenez A, de la Torre AG, Aranda MAG, Palomo A (2007) An XRD study of the effect of the SiO<sub>2</sub>/Na<sub>2</sub>O ratio on the alkali activation of fly ash. *Cem Concr Res* 37(2007):671–679
  22. Duxson P, Fernández-Jiménez A, Provis JL, Lukey GC, Palomo A, van Deventer JSJ (2007) Geopolymer technology: the current state of the art. *J Mater Sci* 42:2917–2933. <https://doi.org/10.1007/s10853-006-0637-z>
  23. Turan C, Javadi A, Vinai R, Shariatmadari N, Farmani R (2020) Use of class C fly ash for stabilisation of fine-grained soils. In *proceedings of the EUNSAT conference, Lisbon, Portugal, 19–21 October 2020*
  24. Cristelo N, Glendinning S, Fernandes L, Pinto AT (2012) Effect of calcium content on soil stabilisation with alkaline activation. *Constr Build Mater* 29(2012):167–174. <https://doi.org/10.1016/j.conbuildmat.2011.10.049>
  25. Abdullah HH, Shahin MA, Walske M (2020) Review of fly-ash-based geopolymers for soil stabilisation with special reference to clay. *Geosciences (Basel)* 10:249. <https://doi.org/10.3390/geosciences10070249>
  26. Singhi B, Laskar AI, Ahmed MA (2016) Investigation on soil-geopolymer with slag, fly ash and their blending. *Arab J Sci Eng* 41(393):393–400. <https://doi.org/10.1007/s13369-015-1677-y>
  27. Singh SP, Chowdhury S, Mishra PN (2015) an experimental investigation on strength characteristics of alkali activated fly ash. *Procedia Earth Planetary Sci* 11(2015):402–409. <https://doi.org/10.1016/j.proeps.2015.06.039>
  28. Sukmak P, Horpibulsuk S, Shen S-L, Chindaprasirt P, Suksiripattanapong C (2013) Factors influencing strength development in clay–fly ash geopolymer. *Constr Build Mater* 47:1125–1136. <https://doi.org/10.1016/j.conbuildmat.2013.05.104>
  29. Correa-Silva M, Araujo N, Cristelo N, Miranda T, Gomes AT, Coelho J (2018) Improvement of a clayey soil with alkali activated low-calcium fly ash for transport infrastructures applications. *Road Mater Pavement Des* 20(8):1912–1926. <https://doi.org/10.1080/14680629.2018.1473286>
  30. Dunga JR, Codilla EET (2018) Fly ash based geopolymer as stabilizer for silty sand embankment materials. *Int J Geomate* 14(46):143–149. <https://doi.org/10.21660/2018.46.7181>
  31. Leong HY, Ong DEL, Sanjayan JG, Nazari A (2018) Strength development of soil-fly ash geopolymer: assessment of soil, fly ash, alkali activators, and water. *J Mater Civ Eng* 30:04018171. [https://doi.org/10.1061/\(asce\)mt.1943-5533.0002363](https://doi.org/10.1061/(asce)mt.1943-5533.0002363)
  32. Ridthirud C, Leekongbub S, Chindaprasirt P (2018) Compressive strength of soil cement base mixed with fly ash – based geopolymer. *Int J Geomate* 14(46):82–88. <https://doi.org/10.21660/2018.46.mat61>
  33. Trinh SH, Bui QAT (2018) Influencing of clay and binder content on compression strength of soft soil stabilized by geo-polymer based fly ash. *Int J Appl Eng Res* 13:7954–7958
  34. Coudert E, Paris M, Deneele D, Russo G, Tarantino A (2019) Use of alkali activated high-calcium fly ash binder for kaolin clay soil stabilisation: physicochemical evolution. *Constr Build Mater* 201(2019):539–552. <https://doi.org/10.1016/j.conbuildmat.2018.12.188>
  35. Debanath, O. C., Rahman, A., Farooq, S. M. (2019). Use of fly ash geopolymer for stabilization of expansive soil. In: 9<sup>th</sup> International Conference on Geotechnique, Construction Materials and Environment. Tokyo, Japan, 20–22 November 2019
  36. Syed M, GuhaRay A, Kar A (2020) Stabilization of expansive clayey soil with alkali activated binders. *Geotech Geol Eng* 38:6657–6677. <https://doi.org/10.1007/s10706-020-01461-9>
  37. Abdullah HH, Shahin MA, Walske ML, Karrech A (2019) Systematic approach to assessing the applicability of fly-ash-based

- geopolymer for clay stabilization. *Canadian Geotech J* 57:1356–1368. <https://doi.org/10.1139/cgj-2019-0215>
38. Miao S, Shen Z, Wang X, Luo F, Huang X, Wei C (2017) Stabilization of highly expansive black cotton soils by means of geopolymerization. *J Mater Civ Eng*. [https://doi.org/10.1061/\(ASCE\)MT.1943-5533.0002023](https://doi.org/10.1061/(ASCE)MT.1943-5533.0002023)
  39. Khadka SD, Jayawickrama PW, Senadheera S, Segvic B (2020) Stabilization of highly expansive soils containing sulfate using metakaolin and fly ash based geopolymer modified with lime and gypsum. *Transp Geotech* 23:100327. <https://doi.org/10.1016/j.trgeo.2020.100327>
  40. Debanath OC, Rahman A, Farook SM, Islam MR (2024) Application of ecofriendly geopolymer binder to enhance the strength and swelling properties of expansive soils. *Adv Civil Eng* 2024:1–14. <https://doi.org/10.1155/2024/9910728>
  41. Dudekula JR, Kumar SA, Chigurupati S (2024) Experimental investigation on geopolymer-stabilized expansive soil. *Mater Today Proc* 103:223–227. <https://doi.org/10.1016/j.matpr.2023.08.268>
  42. Chi M (2015) Effects of modulus ratio and dosage of alkali-activated solution on the properties and micro-structural characteristics of alkali-activated fly ash mortars. *Constr Build Mater* 99:128–136. <https://doi.org/10.1016/j.conbuildmat.2015.09.029>
  43. Krizan D, Zivanovic B (2002) Effects of dosage and modulus of water glass on early hydration of alkali–slag cements. *Cem Concr Res* 32(2002):1181–1188
  44. Wang W, Noguchi T (2020) Alkali-silica reaction (ASR) in the alkali-activated cement (AAC) system: a state-of-the-art review. *Constr Build Mater* 252:119105. <https://doi.org/10.1016/j.conbuildmat.2020.119105>
  45. Yusuf MO, Johari MAM, Ahmad ZA, Maslehuddin M (2015) Impacts of silica modulus on the early strength of alkaline activated ground slag/ultrafine palm oil fuel ash-based concrete. *Mater Struct* 48:733–741. <https://doi.org/10.1617/s11527-014-0318-3>
  46. Gado RA, Hebda M, Lach M, Mikula J (2020) Alkali activation of waste clay bricks: influence of the silica modulus, SiO<sub>2</sub>/Na<sub>2</sub>O, H<sub>2</sub>O/Na<sub>2</sub>O molar ratio, and liquid/solid ratio. *Materials* 13:383. <https://doi.org/10.3390/ma13020383>
  47. Firdous R, Stephan D (2019) Effect of silica modulus on the geopolymerization activity of natural pozzolans. *Constr Build Mater* 219:31–43. <https://doi.org/10.1016/j.conbuildmat.2019.05.161>
  48. Rios S, Cristelo N, da Fonseca AV, Ferreira C (2017) Stiffness behavior of soil stabilized with alkali-activated fly ash from small to large strains. *Int J Geomech* 17(3):04016087. [https://doi.org/10.1061/\(ASCE\)JGM.1943-5622.0000783](https://doi.org/10.1061/(ASCE)JGM.1943-5622.0000783)
  49. BS EN ISO 14688–2, (2018). Geotechnical Investigation and testing—identification and classification of soil. Part 2: Principles for a Classification. British standard institution: London, UK.
  50. Khaled Z, Mohsen A, Soltan A, Kohail M (2023) Optimization of kaolin into metakaolin: calcination conditions, mix design and curing temperature to develop alkali activated binder. *Ain Shams Eng J* 14:102142. <https://doi.org/10.1016/j.asej.2023.102142>
  51. ASTM C618–05, (2005). Standard specification for coal fly ash and raw or calcined natural pozzolan for use in concrete. ASTM International, West Conshohocken, United States, [www.astm.org](http://www.astm.org).
  52. Rafeet A, Vinai R, Soutsos M, Sha W (2017) Guidelines for mix proportioning of fly ash/GGBS based alkali activated concretes. *Constr Build Mater* 147:130–142. <https://doi.org/10.1016/j.conbuildmat.2017.04.036>
  53. Soutsos M, Boyle AP, Vinai R, Hadjierakleous A, Barnett S (2016) Factors influencing the compressive strength of fly ash based geopolymers. *Constr Build Mater* 110:355–368. <https://doi.org/10.1016/j.conbuildmat.2015.11.045>
  54. Turan C, Javadi AA, Vinai R, Russo G (2022) Effects of fly ash inclusion and alkali activation on physical, mechanical, and chemical properties of clay. *Materials* 15(13):4628. <https://doi.org/10.3390/ma15134628>
  55. Phetchuay C, Horpibulsuk S, Arulrajah A, Suksiripattanapong C, Udomchai A (2016) Strength development in soft marine clay stabilized by fly ash and calcium carbide residue based geopolymer. *Appl Clay Sci* 127–128:134–142. <https://doi.org/10.1016/j.clay.2016.04.005>
  56. Mok VW (1967) Effect of density and moisture on consolidation of compacted soil. *Highw Res Board Proc* 4:1–18
  57. BS 1377–5, (1990). Methods of Test for Soils for Civil Engineering Purposes. Compressibility, permeability, and durability tests. BSI Standard Publications: London, UK.
  58. BS 1377–8, (1990). Methods of Test for Soils for Civil Engineering Purposes. Shear strength tests (effective stress), BSI Standard Publications: London, UK.
  59. Abdullah, H. H., Shahin, M. A. (2019). Strength characteristics of clay stabilized with fly-ash based geopolymer incorporating granulated slag. In: Proceedings of the 4th World Congress on Civil, Structural, and Environmental Engineering. Rome, Italy, <https://doi.org/10.11159/icgre19.139>
  60. Ignat R, Baker S, Holmen M, Larsson S (2019) Triaxial extension and tension tests on lime-cement-improved clay. *Soils Found* 59:1399–1416. <https://doi.org/10.1016/j.sandf.2019.06.004>
  61. Phanikumar B (2009) Effect of lime and fly ash on swell, consolidation and shear strength characteristics of expansive clays: a comparative study. *Geomech Geoenviron* 4(2):175–181. <https://doi.org/10.1080/17486020902856983>
  62. Mir B, Sridharan A (2014) Volume change behavior of clayey soil–fly ash mixtures. *Int J Geotech Eng* 8(1):72–83. <https://doi.org/10.1179/1939787913Y.0000000004>
  63. Shil S, Pal SK (2015) Permeability and volume change behaviour of soil stabilized with fly ash. *Int J Eng Res Technol (IJERT)* 4(2):840–846
  64. Chew S, Kamruzzaman A, Lee F (2004) Physicochemical and engineering behavior of cement treated clays. *J Geotech Geoenviron Eng* 130(7):696–706. [https://doi.org/10.1061/\(asce\)1090-0241\(2004\)130:7\(696\)](https://doi.org/10.1061/(asce)1090-0241(2004)130:7(696))
  65. Jaditager M, Sivakugan N (2018) Consolidation behavior of fly ash-based geopolymer-stabilized dredged mud. *J Waterw Port Coast Ocean Eng* 144:06018003. [https://doi.org/10.1061/\(asce\)ww.1943-5460.0000455](https://doi.org/10.1061/(asce)ww.1943-5460.0000455)
  66. Çoçka E (2001) Use of class C fly ashes for the stabilization of an expansive soil. *J Geotech Geoenviron Eng* 128(11):966–966. [https://doi.org/10.1061/\(asce\)1090-0241\(2002\)128:11\(966\)](https://doi.org/10.1061/(asce)1090-0241(2002)128:11(966))
  67. Prabakar J, Dendorkar N, Morchhale R (2004) Influence of fly ash on strength behavior of typical soils. *Constr Build Mater* 18(4):263–267. <https://doi.org/10.1016/j.conbuildmat.2003.11.003>
  68. Phanikumar B, Sharma R (2007) Volume change behavior of fly ash-stabilized clays. *J Mater Civ Eng* 19(1):67–74. [https://doi.org/10.1061/\(asce\)0899-1561\(2007\)19:1\(67\)](https://doi.org/10.1061/(asce)0899-1561(2007)19:1(67))
  69. Seyrek E (2016) Engineering behaviour of clay soils stabilized with class C and class F fly ashes. *Sci Eng Compos Mater* 25(2):273–287. <https://doi.org/10.1515/secm-2016-0084>
  70. Zha F, Liu S, Du Y, Cui K (2008) Behavior of expansive soils stabilized with fly ash. *Nat Hazards* 47(3):509–523. <https://doi.org/10.1007/s11069-008-9236-4>
  71. Kolay P, Ramesh K (2016) Reduction of expansive index, swelling and compression behavior of kaolinite and bentonite clay with sand and class C fly ash. *Geotech Geol Eng* 34(1):87–101. <https://doi.org/10.1007/s10706-015-9930-4>
  72. Mir B, Sridharan A (2013) Physical and compaction behaviour of clay soil–fly ash mixtures. *Geotech Geol Eng* 31(4):1059–1072. <https://doi.org/10.1007/s10706-013-9632-8>
  73. Whitlow R (1996) Basic soil mechanics. Longman, Essex, UK

74. Kassim KA, Chow SH (2000) Consolidation characteristics of lime stabilized soil. *Malays J Civil Eng* 12(1):31–42
75. Horpibulsuk S, Miura N, Bergado DT (2004) Undrained shear behavior of cement admixed clay at high water content. *J Geotech Geoenviron Eng* 130(10):1096–1105. [https://doi.org/10.1061/\(ASCE\)1090-0241\(2004\)130:10\(1096\)](https://doi.org/10.1061/(ASCE)1090-0241(2004)130:10(1096))
76. Kasama K, Zen K, Iwataki K (2006) Undrained shear strength of cement-treated soils. *Soils Found* 46(2):221–232
77. Kamruzzaman AHM, Chew SH, Lee FH (2009) Structuration and destructuration behaviour of cement-treated Singapore Marine Clay. *J Geotech Geoenviron Eng* 135:573–589
78. Subramaniam P, Sreenadh MM, Banerjee S (2015) Critical state parameters of dredged Chennai marine clay treated with low cement content. *Mar Georesour Geotechnol* 34:603–616. <https://doi.org/10.1080/1064119X.2015.1053641>
79. Turan C, Javadi AA, Vinai R (2022) Effects of class C and class F fly ash on mechanical and microstructural behavior of clay soil—a comparative study. *Materials* 15:1845. <https://doi.org/10.3390/ma15051845>
80. Bryson LS, Mahmoodabadi M, Adu-Gyamfi K (2017) Prediction of consolidation and shear behavior of fly ash-soil mixtures using mixture theory. *J Mater Civ Eng* 29(11):04017222. [https://doi.org/10.1061/\(asce\)mt.1943-5533.0002077](https://doi.org/10.1061/(asce)mt.1943-5533.0002077)
81. Porbaha A, Shibuya S, Kishida T (2000) State of the art in deep mixing technology. Part III: geomaterial characterization. *Ground Improv* 3:91–110
82. Luis A, Deng L, Shao L, Li H (2019) Triaxial behaviour and image analysis of Edmonton clay treated with cement and fly ash. *Constr Build Mater* 197:208–219. <https://doi.org/10.1016/j.conbuildmat.2018.11.222>
83. Correa-Silva M, Miranda T, Rouainia M, Araujo N, Glendinning S, Cristelo N (2020) Geomechanical behaviour of a soft soil stabilised with alkali-activated blast-furnace slags. *J Clean Prod* 267:122017
84. Rajak TR, Yadu L, Pal SK (2019) Analysis of slope stability of fly ash stabilized soil slope. *Geotech Appl* 4:119–126. [https://doi.org/10.1007/978-981-13-0368-5\\_13](https://doi.org/10.1007/978-981-13-0368-5_13)
85. Yoobanpot N, Jamsawang P, Poorahong H, Jongpradist P, Likitlersuang S (2020) Multiscale laboratory investigation of the mechanical and microstructural properties of dredged sediments stabilized with cement and fly ash. *Eng Geol*. <https://doi.org/10.1016/j.enggeo.2020.105491>
86. Ma H, Pei C, Li S, Xu S (2024) Performance evaluation and modification mechanism of red clay treated with lignosulfonate. *Int J Civ Eng* 22:1961–1976. <https://doi.org/10.1007/s40999-024-00981-2>
87. Sezer A, İnan G, Yılmaz H, Ramyar K (2006) Utilization of a very high lime fly ash for improvement of Izmir clay. *Build Environ* 41(2):150–155. <https://doi.org/10.1016/j.buildenv.2004.12.009>
88. Todisco MC, Coop MR (2019) Quantifying “transitional” soil behaviour. *Soils Found* 59:2070–2082. <https://doi.org/10.1016/j.sandf.2019.11.014>
89. Fonseca AV, Cordeiro D, Molina-Gomez F (2021) Recommended procedures to assess critical state locus from triaxial tests in cohesionless remoulded samples. *Geotechnics* 1:95–127. <https://doi.org/10.3390/geotechnics1010006>
90. Robin V, Cuisinier O, Masrouri F, Javadi AA (2014) Chemo-mechanical modelling of lime treated soils. *Appl Clay Sci* 95:211–219. <https://doi.org/10.1016/j.clay.2014.04.015>
91. Horpibulsuk S, Liu MD, Liyanapathirana DS, Suebsuk J (2010) Behaviour of cemented clay simulated via the theoretical framework of the structured cam clay model. *Comput Geotech* 37(2010):1–9. <https://doi.org/10.1016/j.compgeo.2009.06.007>
92. Kichou Z (2015). A study on the effects of lime on the mechanical properties and behaviour of London clay. Ph.D. Thesis. London South Bank University, London, UK.

**Publisher’s Note** Springer Nature remains neutral with regard to jurisdictional claims in published maps and institutional affiliations.

Springer Nature or its licensor (e.g. a society or other partner) holds exclusive rights to this article under a publishing agreement with the author(s) or other rightsholder(s); author self-archiving of the accepted manuscript version of this article is solely governed by the terms of such publishing agreement and applicable law.